SKB TECHNICAL REPORT 86-19

Correlation between tectonic lineaments and permeability values of crystalline bedrock in the Gideå area

Lars O Ericsson, Bo Ronge
VIAK AB, Vällingby

November 1986

SVENSK KÄRNBRÄNSLEHANTERING AB
SWEDISH NUCLEAR FUEL AND WASTE MANAGEMENT CO

BOX 5864 S-102 48 STOCKHOLM
TEL 08-665 28 00 TELEX 13108-SKB

CORRELATION BETWEEN TECTONIC LINEAMENTS AND PERMEABILITY VALUES OF CRYSTALLINE BEDROCK IN THE GIEDÅ AREA

Lars O Ericsson
Bo Ronge

VIAK AB, VÄLLINGBY

November 1986

A list of other reports published in this series during 1986 is attached at the end of this report. Information on KBS technical reports from 1977-1978 (TR 121), 1979 (TR 79-28), 1980 (TR 80-26), 1981 (TR 81-17), 1982 (TR 82-28), 1983 (TR 83-77), 1984 (TR 85-01) and 1985 (TR 85-20) is available through SKB.

VIAK AB
LOE/CÖ/1016
038159

CORRELATION BETWEEN TECTONIC LINEAMENTS AND PERMEABILITY VALUES OF CRYSTALLINE BEDROCK IN THE GIEDÅ AREA

Lars O Ericsson
Bo Ronge

VIAK AB
Box 519
162 15 VÄLLINGBY

Vällingby, November 1986

TABLE OF CONTENT

CORRELATION BETWEEN TECTONIC LINEAMENTS AND PERMEABILITY VALUES OF CRYSTALLINE BEDROCK IN THE GIDEÅ AREA

1. BACKGROUND

The geological preinvestigations constitutes an important part of the activities in finding potential sites for repositories of spent nuclear fuel. The localization of the underground caverns are mainly dependent on good stability of the bedrock, low groundwater turnover, high sorptivity capacity for nuclides and stable geological conditions.

An investigation programme, consisting of geological, hydrogeological and geophysical methods are used for the site characterization in order to clarify the mentioned conditions (Ahlbom, Carlsson, Olsson, 1983). Around 10 sites will be investigated before the final choice of repository location.

The occurence of groundwater in fissures and fractures of the bedrock is very essential in the investigations. The hydraulic conductivity is evaluated at different depths in the exploration boreholes. Afterwards, the tectonic interpretation within every site, governs the calculations of the natural groundwater flow pattern.

It is impossible to exactly verify the hydraulic conditions in three dimensions even if a large amount of conductivity measurements are carried out. A generalization has to be made by a statistical approach. Different studies have shown that the specific capacity of wells, transmissivity and packer test data (injection tests) are from a statistically point of view lognormally distributed. (Freeze 1975; Dagan, 1979 and 1981; Warren & Root, 1961; Carlsson, Winberg, Grundfelt, 1983; Gustafson, Åberg, 1985.)

Experiences from several areas in Scandinavia have shown that a tectonic modell can be used where the earth crust has been broken into a fairly regular rhombic block-like pattern (Ericsson, Johansson, 1984; Gustafson, Liedholm, 1984; Nilsson, Ronge, 1985a; Nilsson, Ronge 1985b; Lundgren et al 1985; Lindberg et al 1985; Bolvede et al, 1983). The crust can be considered as being a rigid plate that is overlying a plastic basement. (See Figure 1.1.) Assuming that the greatest principal stress can change its orientation because of the continental drift, one can expect that tension fractures can appear in both the diagonals of the rhomb (Gustafson, 1985; VIAK, 1984). The tectonic model is presented in chapter 3.

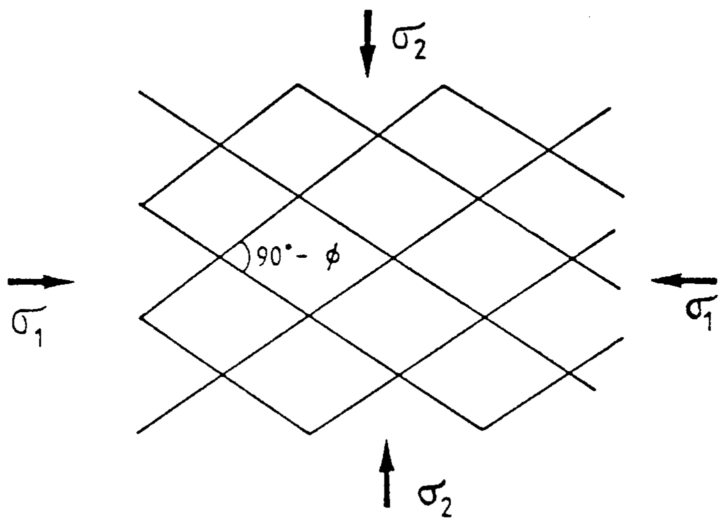

Figure 1.1 If the Mohr-Coulomb failure envelope is applied within a large plate the result will be a rhombic block-line pattern with the longest diagonal parallel to the greatest principal stress orientation. ϕ = angle of internal friction, σ_1 and σ_2 = greatest and least principal stress.

In an area where there exist a lot of information regarding specific yield in wells (discharge capacity per unit of drawdown) or, where a lot of injection tests have been made, it is possible to study the correlation between the described tectonic model and the permeability. Such a study need a careful interpretation of lineaments. This makes it possible to classify the permeability values belonging to shear fractures, tension fractures and undeformed blocks. The manner above has been applied to the Gideå region of Sweden (see figures 1.2, 1.3). A methodology study has been carried out. Permeability values derived from the well archives of the Swedish Geological Survey (SGU) and from former injection tests within the Gideå study site.(See Appendix 1 and 3)

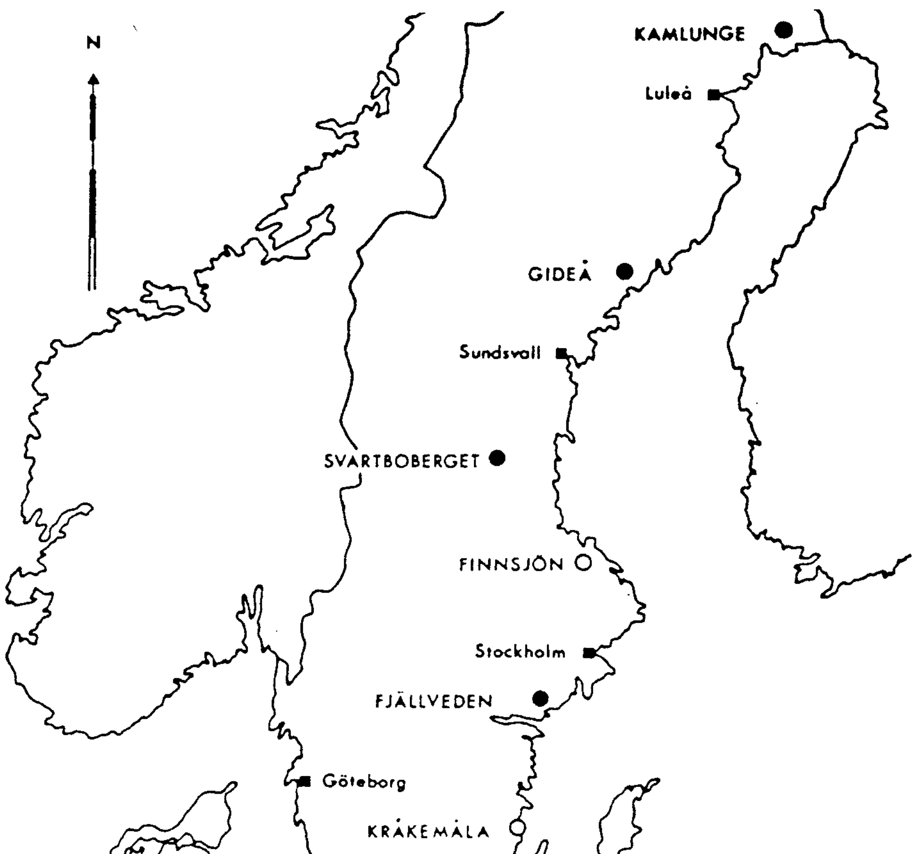

Figure 1.2 Gideå is situated about 500 km north of Stockholm (From Carlsson, Winberg, Grundfelt, 1983)

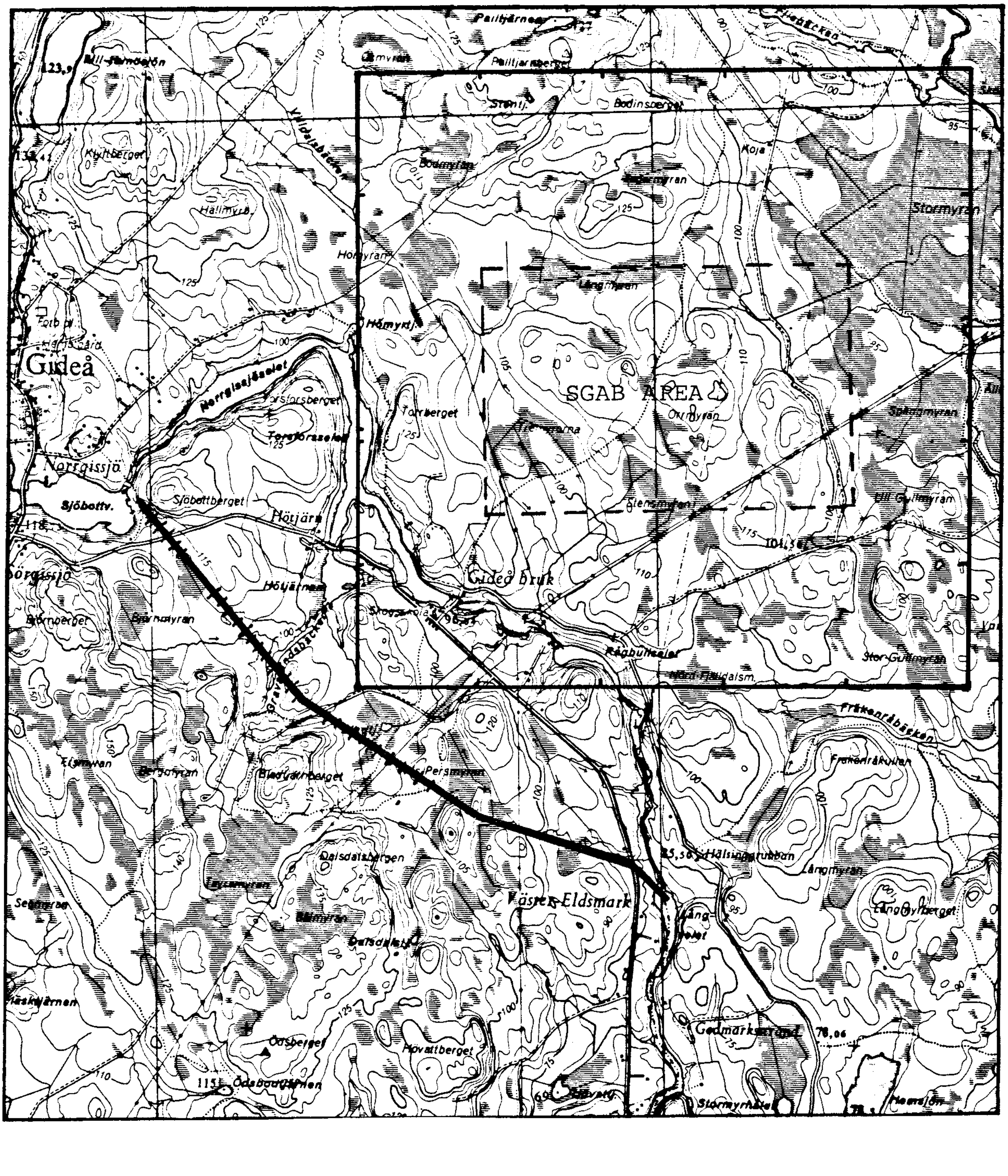

Figure 1.3 Gideå study site. Former investigated area by SGAB. Gissjö hydropower tunnel. Scale 1:50 000

2. GEOLOGICAL CONDITIONS

The Gideå site lies within an rock sequence belonging to the Sveko Karelian orogeny. The bedrock evolution of the region can briefly be described as follows according to Lundqvist, (1985).

The primary rocks in this orogeny were sedimentary rocks of grey wacke composition, which were intruded by a sequence of magmatic rocks ranging from gabbro to granite in composition, the so called primorogenic intrusions. These intrusions also created a folding of the sedimentary sequences together with contact-metamorphic alteration in the vicinity of the intrusions. Due to heat transfer from the magmatic activity all rock types involved were at a later stage altered by regional metamorphism together with further folding.

This metamorphic event created lineation and foliation in the magmatic rocks and a change in mineral composition of the greywacke sequence together with a size of growth in the minerals. In many cases metamorphic differentiation took place giving heavily folded veined gneisses and even to a certain extent migmatites. These migmatites have a granitic composition of the neosome i.e. partial melting of quartz, feldspars and they also have relicts of more mica rich parts of the gneiss still remaining i.e. paleosome.

Regionally the metamorphism led to a complete melting of the greywacke sequence giving a second generation of anatectic massive granites the so called Härnögranites and in some areas pegmatites.

After this period of formation the region around Örnsköldsvik was intruded by a third generation of granites not belonging to the Sveko Karelian orogeny itself, the Revsund granite formation. After this period the magmatic activity ceased for several hundred million years.

During this calm period the deeper parts of the earth crust where the metamorphic and intrusive action had taken place turned over from more plastic to a brittle stage giving raise to the formations of new fracture sets.

Because of this fracturing a new period of magmatic activity took place giving swarms of dolerite dykes in an east-westerly direction. These dykes followed tensional joint sets upwards which are more or less vertical. In the coastal area from Husum and southwards there is a slightly older generation of dolerites following more or less horizontal joints i.e. Ulvödolerites. As mentioned before this is a very brief summary of the geological events and there are in the southern part of this region other events comprising both sedimentary and magmatic rocks which have not been considered since they do not have an impact on the bed-rock geology of the Giteå site.

2.1 Bedrock geology at the Gideå site

The Gideå site area is dominated by rocks originating from the primary greywacke sequence. These rocks varies from well pre-served metagreywackes with sedimentary structures still visible via sedimentary gneisses, veined gneisses to mig- matites. The latter rock types are predominant. In some areas the frequency of pegmatites is quite high. Dolerites appearing in the area are very narrow dykes in an east-westerly direction with a vertical dip. The foliation of the dominating veined gneisses are north-easterly with the dips around 40-50° towards both northwest and southeast due to the folding of the rocks. In the northern part of the investigated area (Drawing 1, Appendix 4), there is a tendency of more east-west strikes of the foliations and a dip around 40° towards south.

Towards the south eastern corner of the investigation area the foliation is in a more northern direction due to heavy folding. Dips in this area are towards north between 40-70°.

3. BRITTLE TECTONIC MODEL

Experiences from a large number of studies (Gustafson et al 1984, Nilsson, Ronge 1985a and 1985b; VIAK 1984) dealing with ground water surveys in crystalline rocks, underground storages and mining operations have given a model for the relationship between different fracture sets and their impact on groundwater flow. The model has been proved to be a versatile tool for calculation of the groundwater flow parameters and to determine main groundwater flow directions in both crystalline and sedimentary fractured rocks.

The model is based upon statistical analyses of a large amount of fracture measurements and there is a need for about 2000 fractures per km^2 in order to get a good statistical background. This value depends on experiences from the projects performed in the mines of Kiruna, Grängesberg and Yxsjöberg (Lindberg et al 1985, Bolvede et al 1983). It has been shown that less than 1000 fractures per km^2 will give difficulties in the interpretation work since the randomly ordered fractures still influence the results.

3.1 Description of the fracture model

The earth crust has as mentioned before, turned over from a plastic stage were the metamorphic processes took place, into a brittle stage were the forces acting on the crust, due to continental movement, can create a brittle fracturing system of joints. When forces are acting upon a block of brittle crust, as seen in fig 3.1, the block will be broken up by a horizontal force along both vertical and inclined joints, fractures.

In fig 3.1.B the block is broken up by two sets of vertical shear fractures and a tensional joint set. This gives a vertical rhombic to square shaped shear fracture pattern depending on the rock-mechanical properties. Gneisses tend to have a more rhombic and granites a more square shaped fracture pattern.

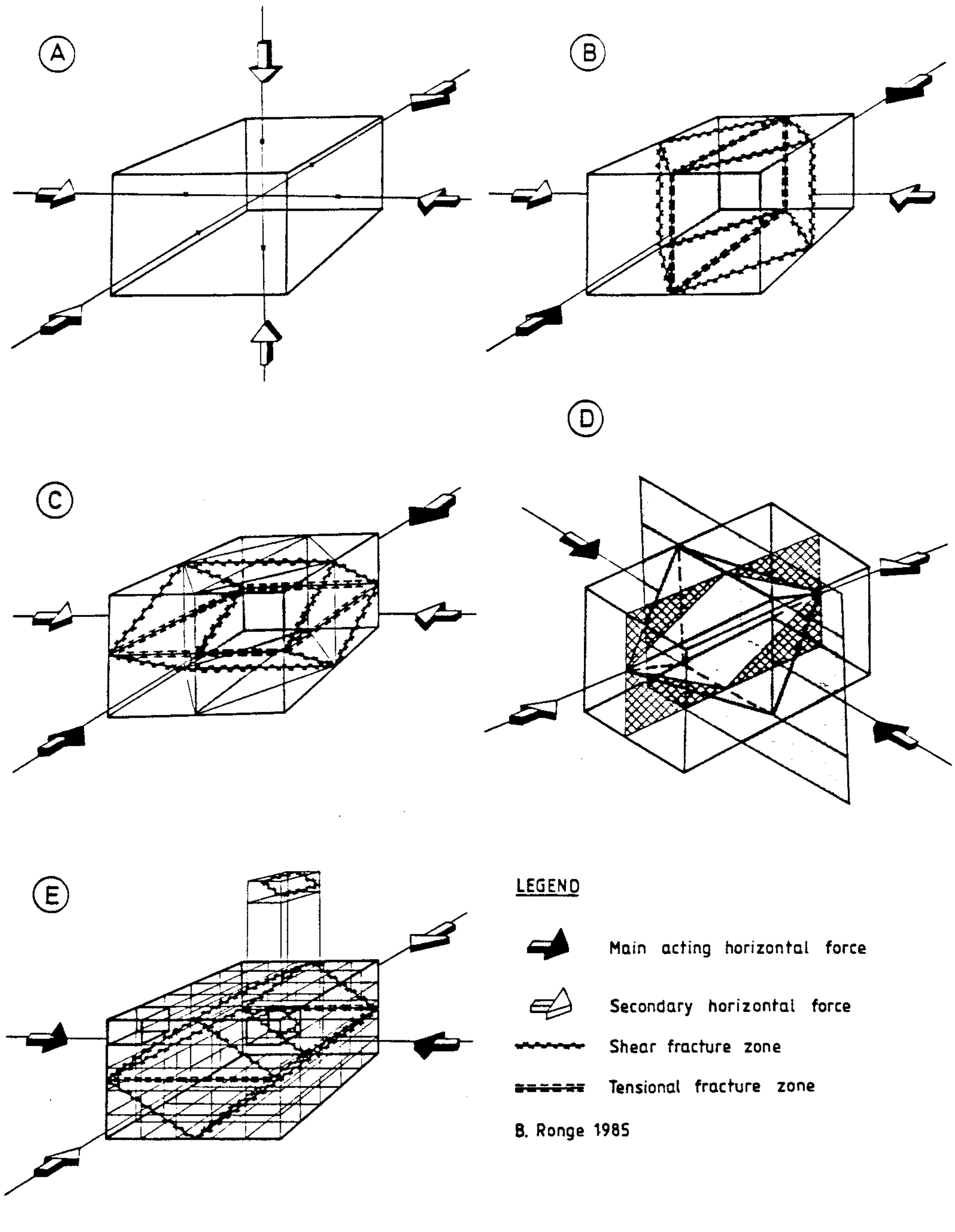

Figrure 3.1 The processes of the brittle tectonic model

Simultaneously with the fracturing in fig 3.1.B there will be inclined shear fractures, as shown in fig 3.1.C, forming a "horizontal" rhomb together with a tensional joint set which is horizontal.

If one put all shear fracture sets together, i.e. vertical and inclined, they will intersect the block giving a bipyramidal polyedron, (see fig 3.1.D).

Since the horizontal forces within the earth crust change direction during the geological time a force acting more or less perpendicular (+/-6^{o}) to the primary one in fig 3.1.B and 3.1.C will divide the bipyramidal polyedron along the plane between the pyramids. This means a new tensional direction is formed in the original vertical rhomb.

Since the rock mass is already fractured the acting force in fig 3.1.D will not create a new set of inclined shears fractures in each unit block. However, if a larger area is studied, traces of a "horizontal" rhomb can be found as demonstrated in fig 3.1.E.

The first steps in de evolution of this model comprised only the sets of vertical shear fractures and the two tensional vertical sets (Gustafson, Ronge, 1981). The blocks formed by the shear fractures has shown to be between 500-800 m in length of each side. Within the blocks itself, the shear fractures directions are found but only for shorter distances.

The second phase of the evolution of this model was established during studies of underground storages facilities and mining operations where it was possible to measure large amounts of inclined fractures which could be statistically treated. These studies has given the final pieces in the framework.

3.2 Presentation of fracture data

There are several ways of presenting fracture data in diagrams. One can use plots on Schmidt stereographic nets or rose diagrams.

In this report we have chosen to present the fracture measurements in rose diagrams (Drawing 2, Appendix 4) and so called "finger" diagrams. The latter diagram is based upon weighted mean values giving a fracture frequency diagram that has proven to be an exellent tool when orientating underground caverns.

In the "finger diagrams" the different fracture sets, essential for the underground construction, can be separated i.e. fractures dipping 70-90° in one group and inclined in an other group.

The "finger diagrams" is shown in fig 3.3.A and .B.

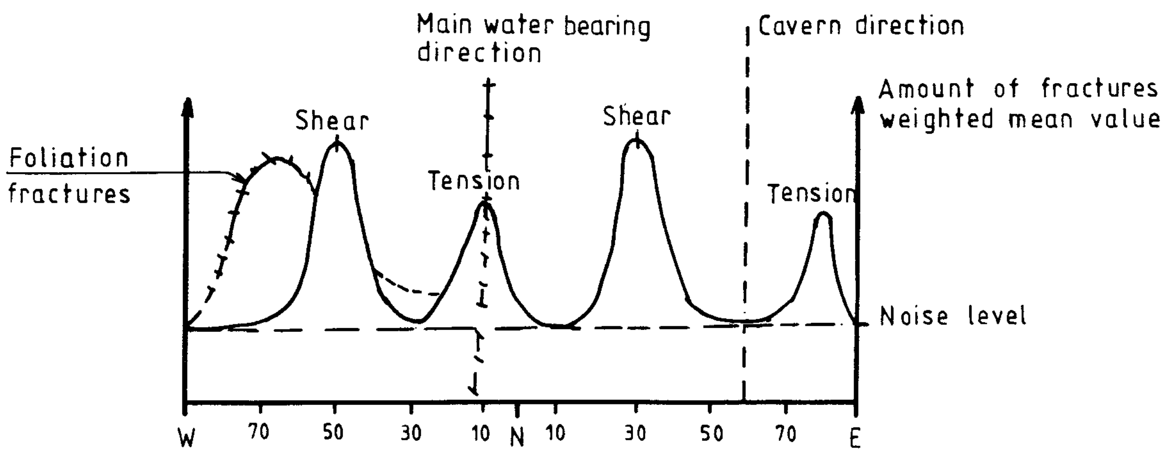

Fig 3.3.A Tentative diagrams showing fractures dipping >70°

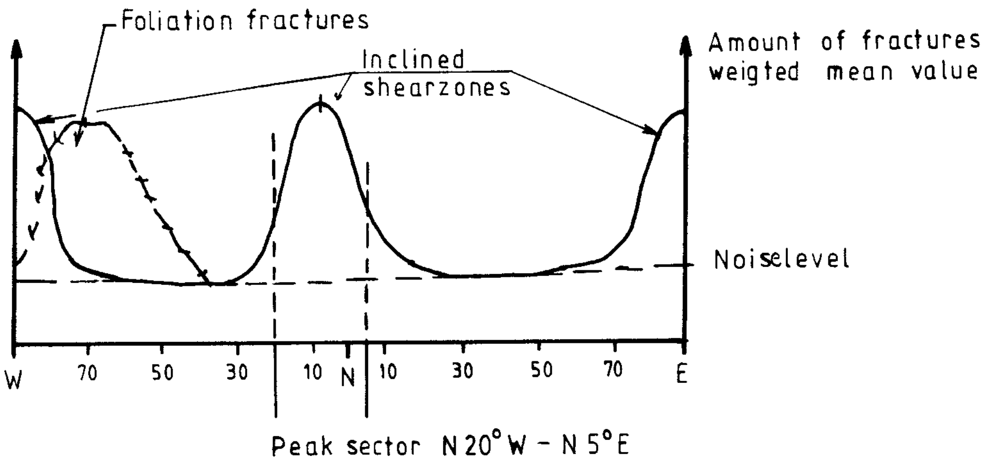

Fig 3.3.B Tentative diagram showing fractures dipping 30-70°

If one gets approximately 2 000 fractures from each square kilometer a diagram can be produced showing the vertical fractures i.e. dip > 70° as in fig 3.3.A. Usually there will be four "fingers" or peaks in such a diagram but in areas with foliated rocks a fifth finger will appear due to foliation fractures. In some cases these foliation fractures can fade out one or two brittle fracture peaks.

As shear fractures are more common the two peaks will often be two to four times higher than tensional fracture peaks. If very few fractures are measured the peaks will be smoothened out and in some cases disappear. Due to foliation the distribution of strike directions of the fractures combined with few measurements will not give any distinct peaks at all. In that case it is difficult to reach above the "noise level" with few scattered fractures.

However, with a sufficient amount of fractures the peaks in the "finger diagram" have proven to fit very close to lineaments drawn from aerial photos or from geophysical investigations.

Since the finger diagrams for dips 30-70°, fig 3.3.B only give an indication on strike directions this information must be supplemented with rose diagrams showing the dips in each peak sector (see fig 3.4).

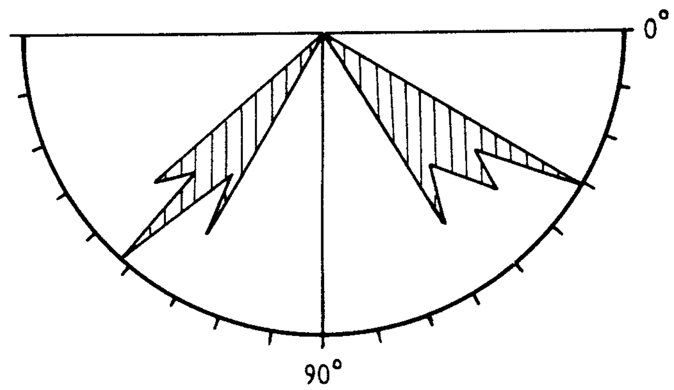

Fig 3.4 Tentative rose diagram showing distribtion of dips within a peak sector strike N20°W-N5°E, from fig 3.3.B

As shown in fig 3.1 there is also a set of more or less horizontal fractures dipping less than 20° in the horisontal rhomb. These fractures are the tensional fractures to the rhomb and are very scarcely occuring in the bedrock outcrops. In very deep mining shafts they occur in swarms at certain levels. This is quite natural if one look at a unit rhomb with a side of 800 m. The horizsontal tensional fracture sets ought to be repeated roughly every 500 to 1 100 m downwards, depending on the dip of the inclined shearzones. (In this case dipping in the range between 30° and 60°.)

4. RESULT OF FRACTURE MEASURING

The Gideå study site has been extended in comparison with the area in the SGAB reports which cover 2 x 3 km. This extension, 5 x 5 km, has been done in order to get a better picture of the fracture pattern and to get a larger amount of fractures that could be used for statistical analysis.

The fracture measurements have been done in two different steps. The first step is covering fractures measured on outcroups within the 5 x 5 km area. (See Drawing 1, Appendix 4.) All together these measurements gave 13 483 fracture determinations over an area of 25 km^2 i.e. 540 fractures/km^2. Considering the large coverage of overburden in the area this amount must be satisfactory. Since fracture measurements of flat lying outcrops give an overrepresentation of vertical to steep fractures a second step of measurements have been performed in a tunnel system under construction from lake Gissjön along the river Gideälv. This second step comprises 4194 fracture determinations.

4.1 Fracture mapping of outcrops

In order to evaluate the different fracture sets, mapped in the outcrops within the 5 x 5 km area, one has to reduce the measure ments with fractures coinciding with the foliation. As shown in fig 4.1 the foliation fractures has a maximum around N 50 ^{o}E +/ /-30^{o} which means that any other fracture set direction within this sector will be extincted or distorted.

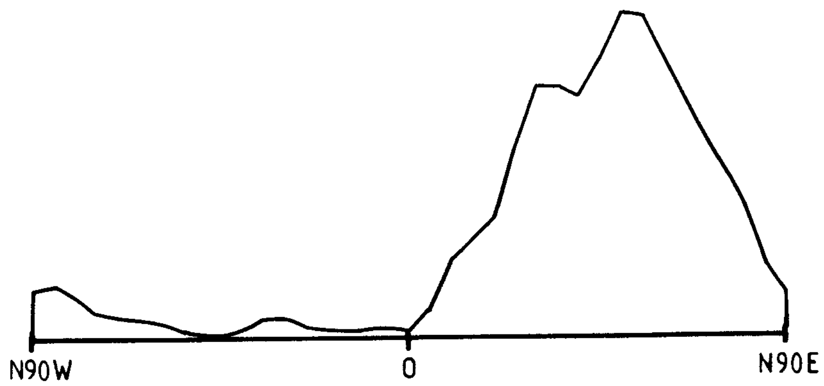

1171 Fractures
105 Fractures correspond to maximum peak

Figure 4.1 Foliation fractures and fractures deviating 5° from the foliation

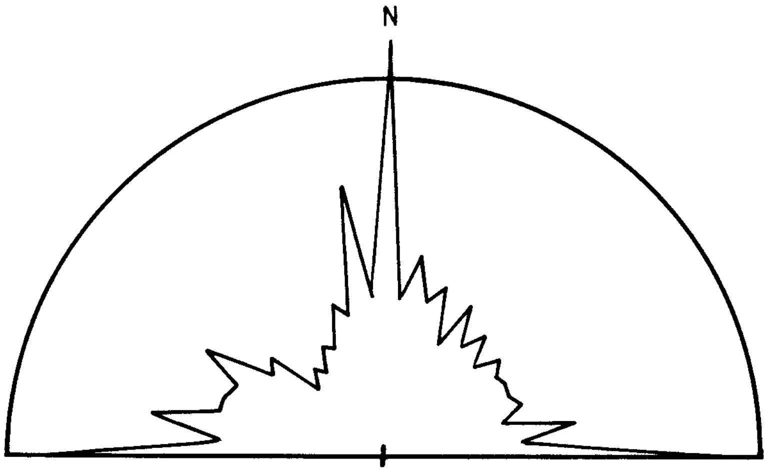

13138 Fractures
838 Fractures correspond to radius

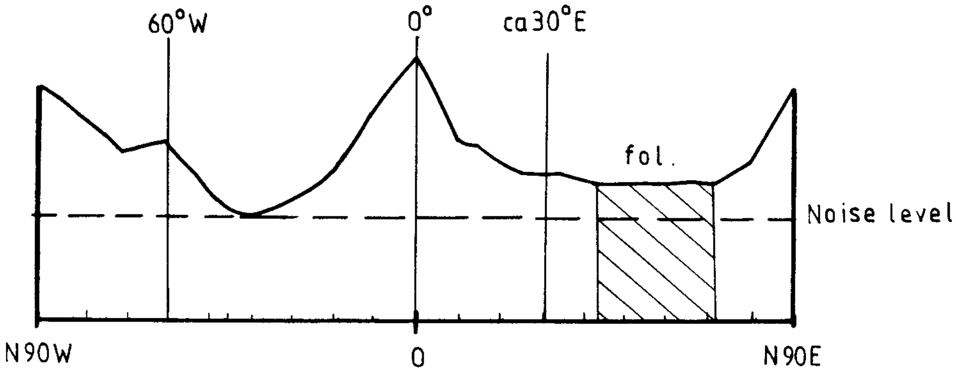

13138 Fractures
591 Fractures correspond to maximum peak

Figure 4.2 Total amount of fractures dipping 70°-90°
No reduction for foliation fractures

In fig 4.2 all fractures dipping more than 70° have been plotted without reduction. In these diagrams three peaks can be distinguished E-W, N 60 °W, N-S. There is a very small peak in N 30° E but it is within the foliation fracture direction and is therefore extincted. After reduction the diagrams change very little as seen in fig 4.3 and the N 30 °E direction is still effected by the foliation fracture sets. Looking at fracture sets inclined 0-65° the amount of measured fractures is 354 which is a to small amount to give a good prognosis. In figure 4.4 the diagrams for 0-65° dip are shown and it is possible to recognize several different peaks.

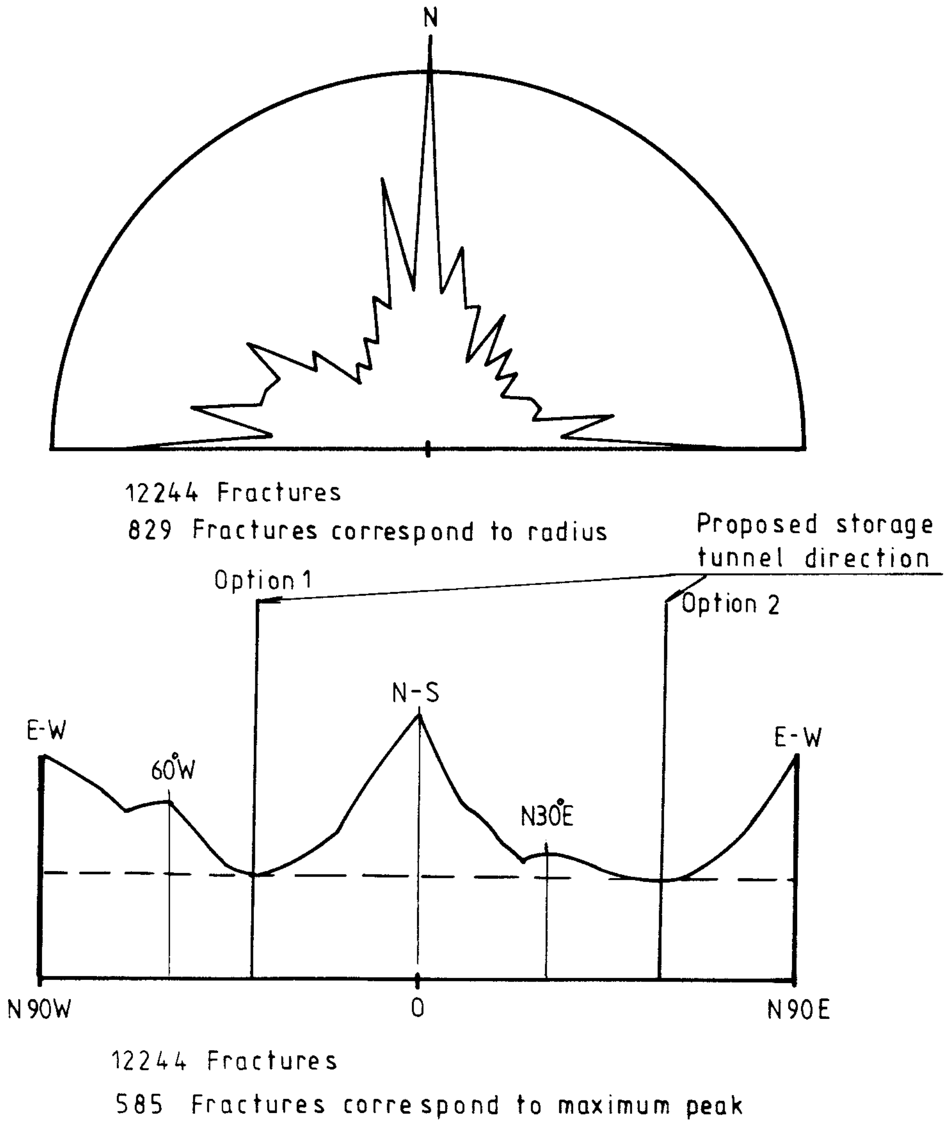

Figure 4.3 Total amount of fractures dipping 70°-90° reduced by fractures parallell to the foliation

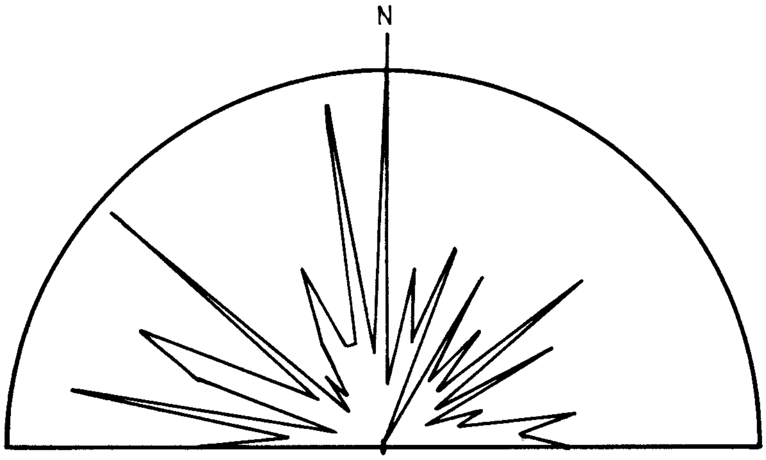

354 Fractures
25 Fractures correspond to radius

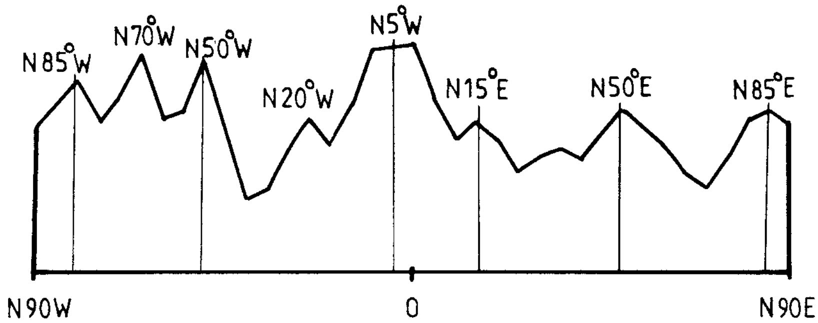

354 Fractures
15 Fractures correspond to maximum peak

Figure 4.4 Total amount of inclined fractures (0^o-65^o)

As seen on Drawing 2 (Appendix 4), where the rose diagrams for each square kilometer are plotted, there is a difference between these diagrams within 5 x 5 km area. These differences is depending on the monitoring of the fractures due to the foliation in the veined gneisses. If the 5 x 5 km area is divided in four equal parts, the fractures in each part can be compiled in diagrams. The result is shown in fig 4.5, 4.6, 4.7 and 4.8. Of these diagrams, fig 4.6 and 4.7 show the most by foliation undisturbed fracture pattern dipping more than 70^o. From these figures it is evident that there exist four peaks E-W, N 60 ^{o}W, N-S and N 30 ^{o}E in the north east and south west quarters. In the north western quarter the N-S and E-W fracture sets are dominating.

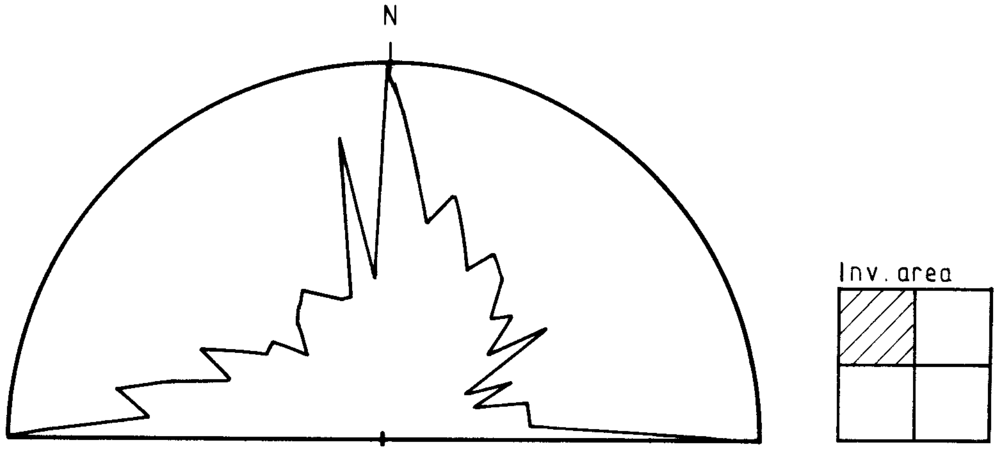

2857 Fractures
159 Fractures correspond to radius

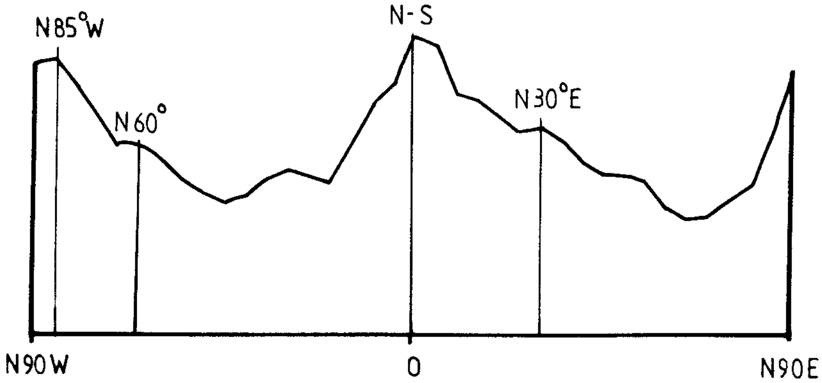

2856 Fractures
126 Fractures correspond to maximum peak

Figure 4.5 Northwest quadrangle, 70°-90° dip.
Reduced by foliation fractures

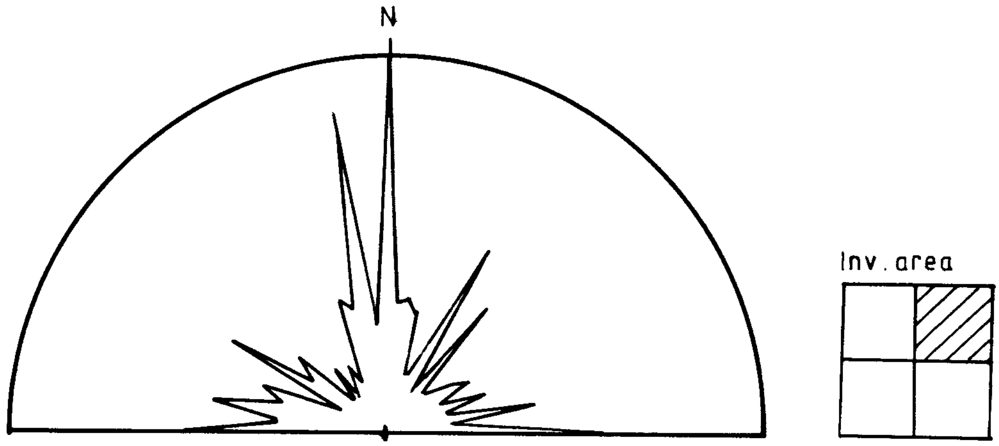

1942 Fractures
176 Fractures correspond to radius

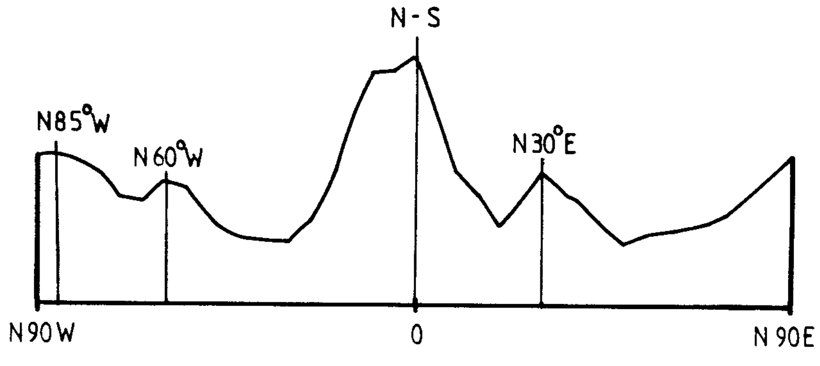

1921 Fractures
113 Fractures correspond to maximum peak

Figure 4.6 Northeast quadrangle, 70°-90° dip.
Reduced by foliation fractures

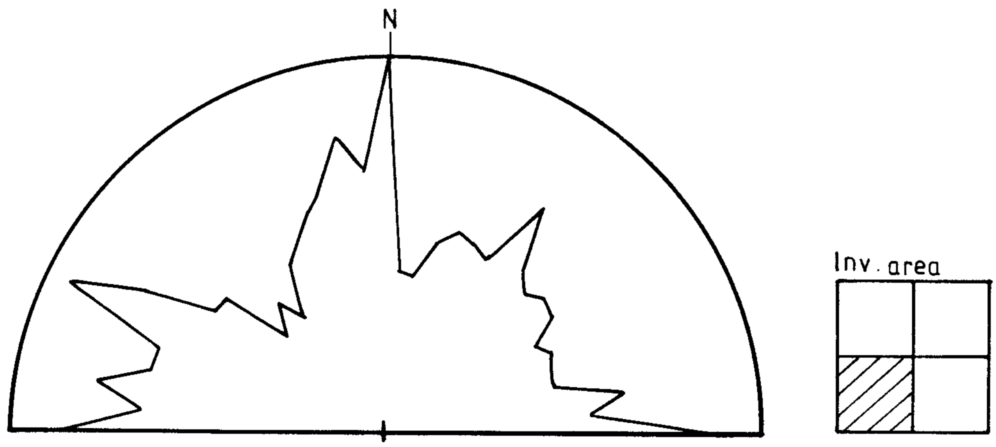

2721 Fractures
128 Fractures correspond to radius

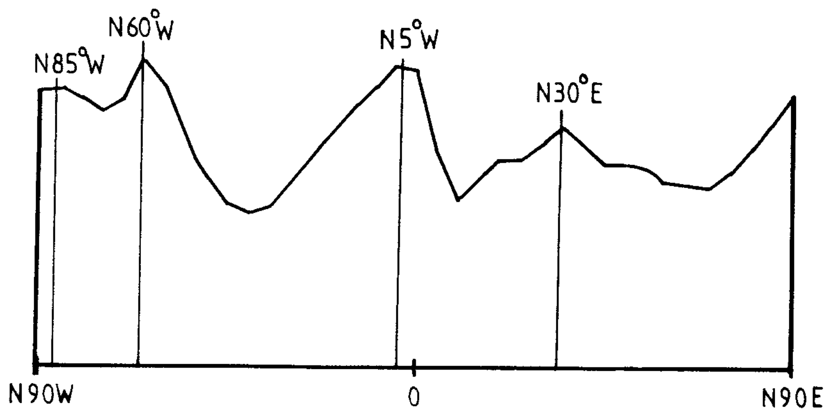

2721 Fractures
103 Fractures correspond to maximum peak

Figure 4.7 Southwest quadrangle, 70°-90° dip.
Reduced by foliation fractures

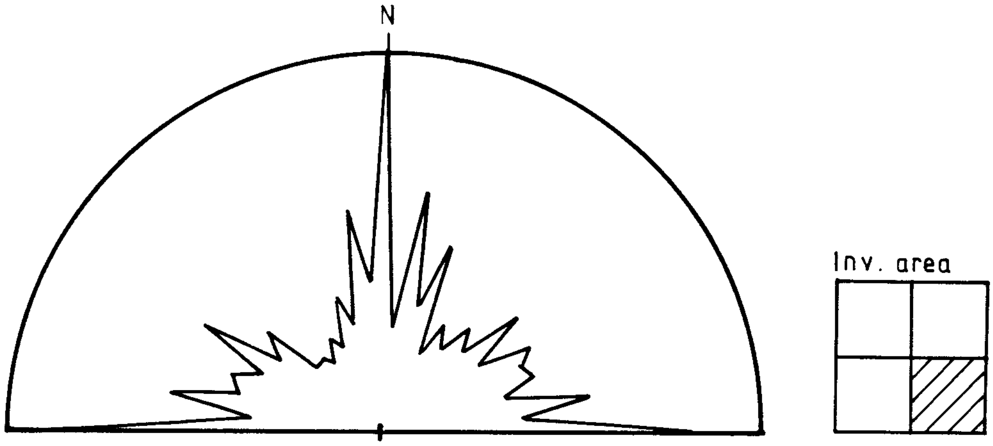

5604 Fractures
382 Fractures correspond to radius

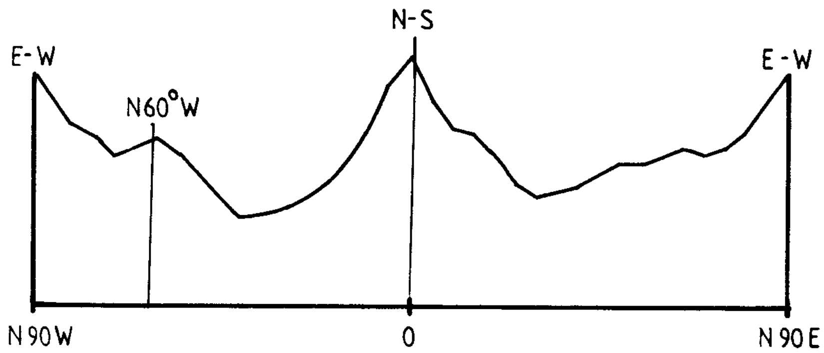

5604 Fractures
253 Fractures correspond to maximum peak

Figure 4.8 Southeast quadrangle, 70°-90° dip
Reduced by foliation fractures

Comparing the results given by the diagrams fig 4.6 and 4.7 and interpretation of regional and local lineament directions there is an extremely good fit between fracture maximum peaks (dip >70°) and the lineament directions.

It is therefore possible to define four essential directions E-W, N 60 °W, N-S and N 30 °E as being lineament fracture mean directions. Of these directions the E-W and N-S are the tensional. The other two directions N 60 °W and N 30 °E are shear directions. The base for this point of view is among other things, earlier experience, the presence of the dolerite dykes in the E-W direction, and that the N 60 °W direction is the major direction more or less for the large vallys from the Kaledonian mountains range down to the Gulf of Bothnia.

4.2 Fractures mapped in Gissjö hydropower tunnel

In the tunnel area it was possible to distinguish the same four main directions as mentioned above (see Drawing 3, Appendix 4). In order to show the dip of the fractures belonging to these four sets, a modified rose diagram has been made. As seen in Drawing 4 (Appendix 4) the central diagram is an ordinary rose diagram showing the strike of the four main directions. Each direction covers a sector of approximately 30°. The dips of the fractures belonging to the sector have been plotted. It is evident that in the N-S tensional sector the vertical fractures are outstanding compared to the inclined ones. An enlargement has been done around the origopoint and the result shows that there are inclined fracture sets differing 20° from the vertical line which is quite normal.

The East-West tensional direction is connected to a more dominant set of inclined fractures according to the earlier described model.

The directions N60 ^{o}W and N30 ^{o}E show tendencies of inclined fractures around a dip of 40-60^{o} which in most cases could be explained by foliation fractures which have been opened by the blasting in the tunnel.

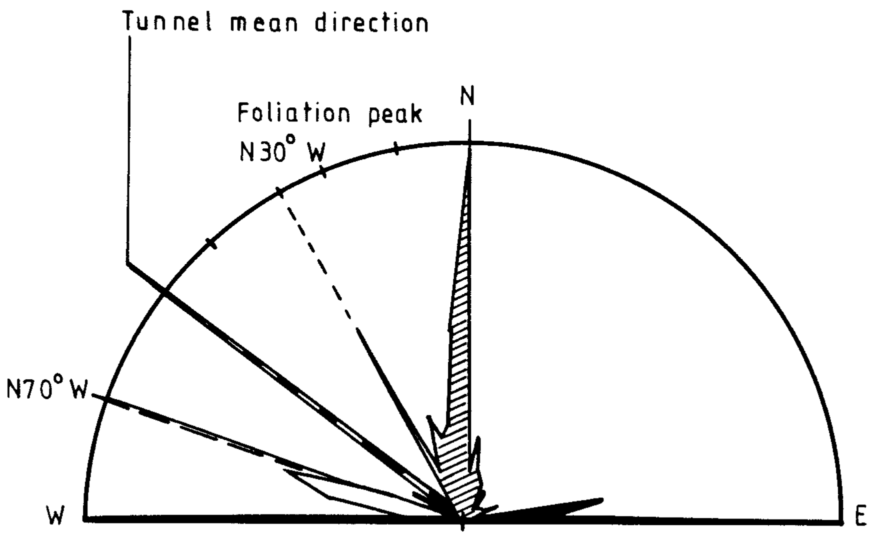

2092 Fractures
274 Fractures correspond to radius

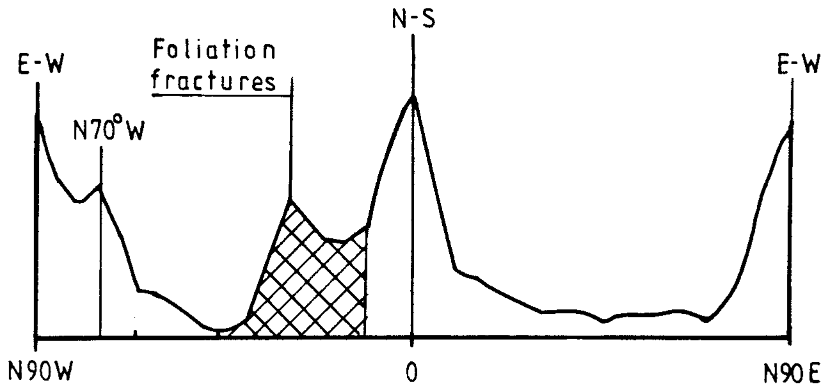

2092 Fractures
179 Fractures correspond to maximum peak

Figure 4.9 Fracture measurements in the Gissjö hydropower tunnel. Dip 70-90^{o}

Looking at the distribution of vertical fractures in the different sectors it is obvious that the tensional sets E-W respectively N-S are dominant over the shear directions.
Comparing the two tensional sets the N-S direction dominantes over the E-W at a ratio of approximately 4:1.

The shear sets are more or less equally distributed perhaps with a more dominating direction in N60 °W when taking into account the tunneldirection, see fig 4.9 and 4.10. The tunneldirection lies more or less perpendicular to the N30 °E direction, which should mean that this direction ought to be more dominant with more fractures cutting the tunnel. The N60 °W sector is more or less parallel to the tunnel direction and as seen in Drawing 4 the amount of fractures in this sector is higher. This can be explained, on the other hand, by the fact that the lineaments in N60 °W, giving the direction of the Gissjö lake, and partly the river Gideälven, are in the tunnel area outnumbering all other shear directions. This means when a site is positioned close to a major fault line (lineament) this fracture set direction will outnumber all other directions of fracture sets present. Looking at the Gideå area it is possible to differ between larger and smaller faultzones. The larger ones are parallel to the major rivers in the area such as Gideälven, Flisbäcken, Saluån, Husån etc. These rivers are either following an approximately N60 °W or a N-S direction. Only at a few positions the N30 °E direction is visible. The E-W direction is further more scarce than the N30 °E direction.

For the evaluation of the hydraulic properties within the Gideå area the following strikes and dip should be used (see Drawing 5):

1. N60°W +/- 15° dip vertical (shear)
2. N30°E +/- 15° dip vertical to 70°NW (shear)
3. N-S +/- 15° dip vertical (tension)
4. E-W +/- 15° dip vertical to 70°N (tension)

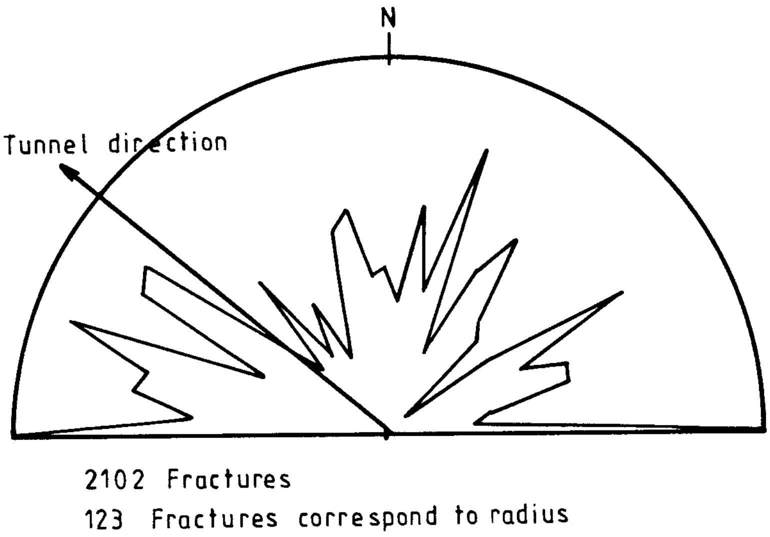

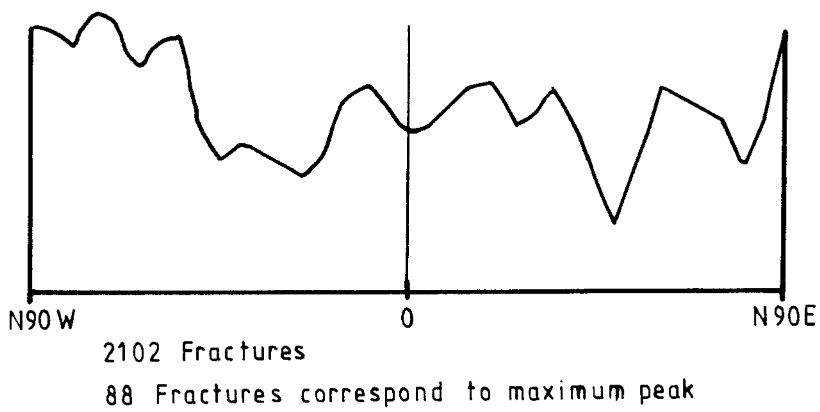

Fig 4.10 Fracture measurements in the Gissjö hydropower tunnel. Dip 0-65°

4.3 Magnetic and Slingram anomalies

SGAB has produced two anomaly maps over the Gideå site, one "slingram 18kHz" and one magnetic-total intensity.

From the magnetic anomaly map it is possible to distinguish the east-westerly dolerites which coincide with the lineament directions found. Except dolerites there are other high magnetic areas in this east-westerly direction. It is also possible to fit both N60°W and N30°E lineament directions to magnetic higher areas or zones (see Drawing 6).

By using the "slingram 18kHz" anomaly map (Drawing 5) there is quite good fit to lineaments found in the area. There is a good fit to both shear and tensional directions. The more prominent directions are the tensional ones in N-S and E-W. Of the shear directions the N60°W is dominant compared with the N30°E.

5. GENERAL HYDROGEOLOGICAL ASPECTS ON TECTONICS

Former investigations have shown a significant higher median specific capicity for drilled wells in or near tension fractures compared to wells in or near shear fractures and compared to wells in undeformed parts of bedrock blocks (Ericsson, Johansson, 1984). Tension fractures represent in other words the most important water bearing zones in bedrock. However, the shear zones constitute the most conspicuous lineaments in the landscape and they are comparatively easy to observe. In hydrogeological investigations it is therefore essential to make a proper methodic surveying of fissures, fractures and foliation in the bedrock.

As some groups of fractures conduct water better than others it implies that crystalline bedrock in most cases represents an anisotropic medium. This results in elliptical drawdown cones in the bedrock in case of a discharge from a well or in case of a leakage to a cavern. The major axis of the ellipse is parallel to one of the two tensional directions. This can also be connected to the stress situation in the rock. Due to the existing force, one set of tension fractures will be open and the other will be more closed. Experiences from the construction of the heat storage cavern at Lyckebo, Uppsala, showed an elliptical drawdown cone in the surrounding bedrock. The major axis of the ellipse was parallel to the greatest principal stress parallel to the most water conducting tension fractures (Gustafson, Liedholm, 1984).

6. EVALUATION OF HYDRAULIC DATA

6.1 Hydraulic conductivity in boreholes at the Gideå site

In Gideå 11 coredrillings have been used for water injection tests. In total 289 sections of 25 m have been evaluated. The sections were sealed off by rubber packers. Futhermore, some investigations have been performed on 5 and 10 m sections. A description of the transient tests as well as the evaluation methods are presented by Carlsson, Winberg, Grundfelt (1983). (See Appendix 3)

6.2 Specific capacity from SGU Well archives

At the well archives of SGU, discharge capacities (Q) are registered for thousands of wells which are drilled in crystalline bedrock. Usually the borehole depths (d_w) and the static groundwater levels (d_o) of the wells are also registered. The estimation of the discharge capacity is made by emptying the boreholes by air-lift pumping. After that, the drillers record the rate of the water level rise in the hole. For short recovery periods the specific capacity (Q/s_w) can be derived from

$$Q/s_w = Q/(d_w - d_o) \qquad (s_w = \text{drawdown})$$

If the skin effects are neglected it can be shown that a generalized value for the transmissivity, T, in the surroundings of a borehole is $T \approx 1,4 \cdot (Q/s_w)$. (See Gustafson 1985.) This means that an approximately value of the transmissivity can be estimated by help of the data from the well archives. The advantage of the archives data is the large amount of values which can be statistically treated and not the accurancy of the single well estimated value.

Discharge capacities from wells within the topographic maps 19J NW, 19J NE, 20J SW, 20J SE, have been statistically treated in this study. The drawdown, s_w, caused by the air-lift pumping, is assumed to be equal to the borehole depth. I.e. the distances from the surface to the groundwater levels is considered to be neglected compared to the total depths of the boreholes.

7. REGIONAL CORRELATION BETWEEN ROCKS, TECTONIC LINEAMENTS AND SPECIFIC CAPACITY OF WELLS

A tectonic model has been constructed by help of the fracture surveying, the existing geophysical investigations and the topographical conditions. The model covers the topographic maps 19J NW, 19J NE, 20J SW and 20J SE. Within these maps 163 wells are registered (1/7 1985) at the SGU well archives.(See appendix 1.)

At the well archives there are data of wells which are more or less professionally preinvestigated and sited. Most wells are drilled before 1980, when the VLF-technique was not so very common. In the statistical approach the well data are treated as being random samples of the populations (rock type, tectonic family).

Statistical analysis has been made according to the tectonic lineaments and type of rock. Separate maps in scale 1:50.000, with plotted wells have been delivered from the SGU. The tectonic intepretation has been implemented on topographic maps, also in scale 1:50.000. If a center of a well mark on a map has been situated within a distance of approx. 100 m (2 mm on map) from an interpretated tectonic lineament, the well has been regarded as corresponding to the interpretated tectonic "family" respectively. The interpretated tectonical environment of the wells and the corresponding rock type is shown in appendix 1. It was earlier mentioned that features like the specific capacity can be considered as lognormally distributed. This means that the relative frequences of the individual objects tend to be concentrated towards low values and that high values are scarce. If the specific capacities are made in a logarithmic form they will form a straight line on a normal probability paper if the sample is undisturbed by limits in measuring ranges. The plotting position is used according to the Samsioe--Kivisild formula.

Wells which are situated in soil, and bedrock wells without any discharge estimation have been excluded in the statistical analysis. In total they are 17.

Table 7.1 presents the different samples, the determined geometric mean $\bar{X}$ (ideal = median value) and the estimate of the standard deviation regarded as $\widehat{\log \sigma} = \log s\sqrt{n/(n-1)}$.

The 90%, 95% and 99% confidence intervals for the geometric mean values of the populations are also presented in the table. The diagrams in appendix 2 show the adjusted lognormal distributions.

The standard deviations of all the populations are unknown. In cases where the amount of wells don't exceed 30 the confidence intervals for the geometric means have been determined by using the t distribution.

It may be considered that the values of the specific capacity represent the conductivity from surface down to a depth of 150 m.

From Table 7.1 it can be noticed that the deviation within the samples, $\widehat{\log \sigma}$, is large.

Regarding the tectonic conditions, the sample of tension fractures plus the crosspoints have a mean of 28,2 l/h, m. This is about 3 times higher than those of the shear zones and the undisturbed blocks. The confidence intervals also confirm that the tension fractures generally seen have a higher conductivity than the shear zones and the undeformed parts of the blocks.

Among the rocks the dolerite, laccolith form and not dikes, shows the lowest conductivity. From a regional point of view the migmatite and sediment gneisses have in average the same conductivity as the granites (old and young).

The Gideå area is situated about 30 km from the shoreline of the Gulf of Bothnia. If one compares the more coastal "migmatite" wells (19J NE + 20J SE) to those in the west of the region (19J NW + 20S SW) it is found that the specific capacity in average is higher at the coast (17,0 l/h, m) than inland (10,5 l/h,m). The reason for this result is the more intensive tectonic activity along the north-southern fracture planes in the coastal area.

TABLE 7.1 Results of statistical analysis concerning specific capacity values (litres/hour, meter) of bedrock well. Correlation to tectonics and rock types

Sample	Number of wells n	Geom mean $\bar{x}$	Confidence interval for geometric mean 90%	95%	99%	Estimate of stand dev $\log \hat{\sigma}$
Total	146	12,9	10,5-15,9	10,2-16,2	9,3-17,8	0,63
Tens +						
Crossp.	45	28,2	20,9-38,0	19,5-40,7	17,4-45,7	0,51
Shear	38	7,2	4,8-11,0	4,4-12,0	3,7-14,1	0,65
Block	63	10,5	7,8-14,1	7,4-14,8	6,5-17,0	0,61
Dolerite	14	5,5	2,8-11,0	2,4-12,6	1,7-17,4	0,59
Y.granite	17	15,5	10,2-23,4	9,6-25,1	8,1-29,5	0,41
Migmatite	98	14,1	11,0-18,2	10,2-19,5	9,3-21,4	0,68
O.granite	9	10,5	3,8-28,9	3,0-36,3	1,7-63,1	0,64
Granites	26	13,5	9,1-20,0	8,3-21,9	7,1-25,7	0,50
Migm east	64	17,0	12,0-24,0	11,2-25,7	9,8-29,5	0,72
Migm west	33	10,5	7,1-15,5	6,5-17,0	5,5-20,0	0,58

8. CORRELATION BETWEEN TECTONIC LINEAMENTS AND HYDRAULIC CONDUCTIVITY AT THE GIDEÅ SITE

A tectonic model has been constructed by help of the fracture surveying, the slingram anomalies, the magnetic anomalies and the topographical conditions. The model covers an area of 6 square kilometres (Scale 1:5 000). Within this area core drillings and percussion drillings have been made. In 11 of the core drillings 289 injection tests have been performed in 25 m sealed off sections. (See Drawing 5, Appendix 4.)

Statistical analysis have been made according to the tectonic lineaments. It is considered that the vertical lineaments found in the tectonic interpretation are most essential with respect to the water bearing conditions. The conductivity values have been graphically classified into four samples. (See Drawing 5) The values are belonging to:

- Tension fractures N-S T1
- Tension fractures E-W T2 (and dolerite dikes)
- Shear fractures
- Undeformed parts of the blocks
  (In the following called, Blocks)

Further on, these values have been distributed into three depth categories. Fractures belonging to dephts at:

- 0 - 50 m
- 50 - 200 m
- >200 m

The conductivity data and the classification are presented in Appendix 3.

As mentioned before, the conductivity values in logaritmic form, will result in a straight line if they are plotted in a normal probability paper. The plotting position is used according to the Samsioe-Kivisild formula. The number of values differ a lot within the samples:

	0-50 m	50-200 m	>200 m	Total
Tension 1	1	7	18	26
Tension 2	1	6	28	35
Shear zones	1	4	10	15
Blocks	14	58	141	213

Due to low hydraulic conductivity a lot of data show results below the performance boundary of the measuring equipment. The only way to compare the different data is to graphically determine the characteristic parameters from a plot in a probability paper. (Gustafson, Liedholm, 1985)

From the storage point of view it is most interesting to analyse the conditions at dephts more than 200 m. Figure 8.1 shows the adjusted lognormal distributions. Table 8.1 presents the graphically determined mean value $\bar{X}$ and the estimate of the standard deviation regarded as $\log\hat{\sigma} = \log s\sqrt{n/n-1}$. The 90%, 95% and 99% confidence intervals for the geometric mean values of the populations are also presented in the table.

TABLE 8.1 Results of statistical analysis concerning hydraulic conductivity values (m/s) at depths >200 m. Correlation to tectonics at the Gideå site

Sample	Number of values	Geom mean	Confidence interval for geometric mean			Estimate of stand-dev
	n	$\bar{X}$	90%	95%	99%	$\log\hat{\sigma}$
Tens 1	18	$1,4\cdot10^{-11}$	$2,6\cdot10^{-12}-7,5\cdot10^{-11}$	$1,8\cdot10^{-12}-1,1\cdot10^{-10}$	$8,4\cdot10^{-13}-2,3\cdot10^{-10}$	1,8
Tens 2	28	$7,0\cdot10^{-10}$	$1,7\cdot10^{-10}-2,8\cdot10^{-9}$	$1,3\cdot10^{-10}-3,8\cdot10^{-9}$	$7,3\cdot10^{-11}-6,7\cdot10^{-9}$	1,9
Shear	10	$8,0\cdot10^{-12}$	$7,6\cdot10^{-13}-8,3\cdot10^{-11}$	$4,4\cdot10^{-13}-1,5\cdot10^{-10}$	$1,2\cdot10^{-13}-5,2\cdot10^{-10}$	1,7
Blocks	141	$2,9\cdot10^{-11}$	$1,3\cdot10^{-11}-6,5\cdot10^{-11}$	$1,1\cdot10^{-11}-7,5\cdot10^{-11}$	$8,1\cdot10^{-12}-1,0\cdot10^{-10}$	2,5

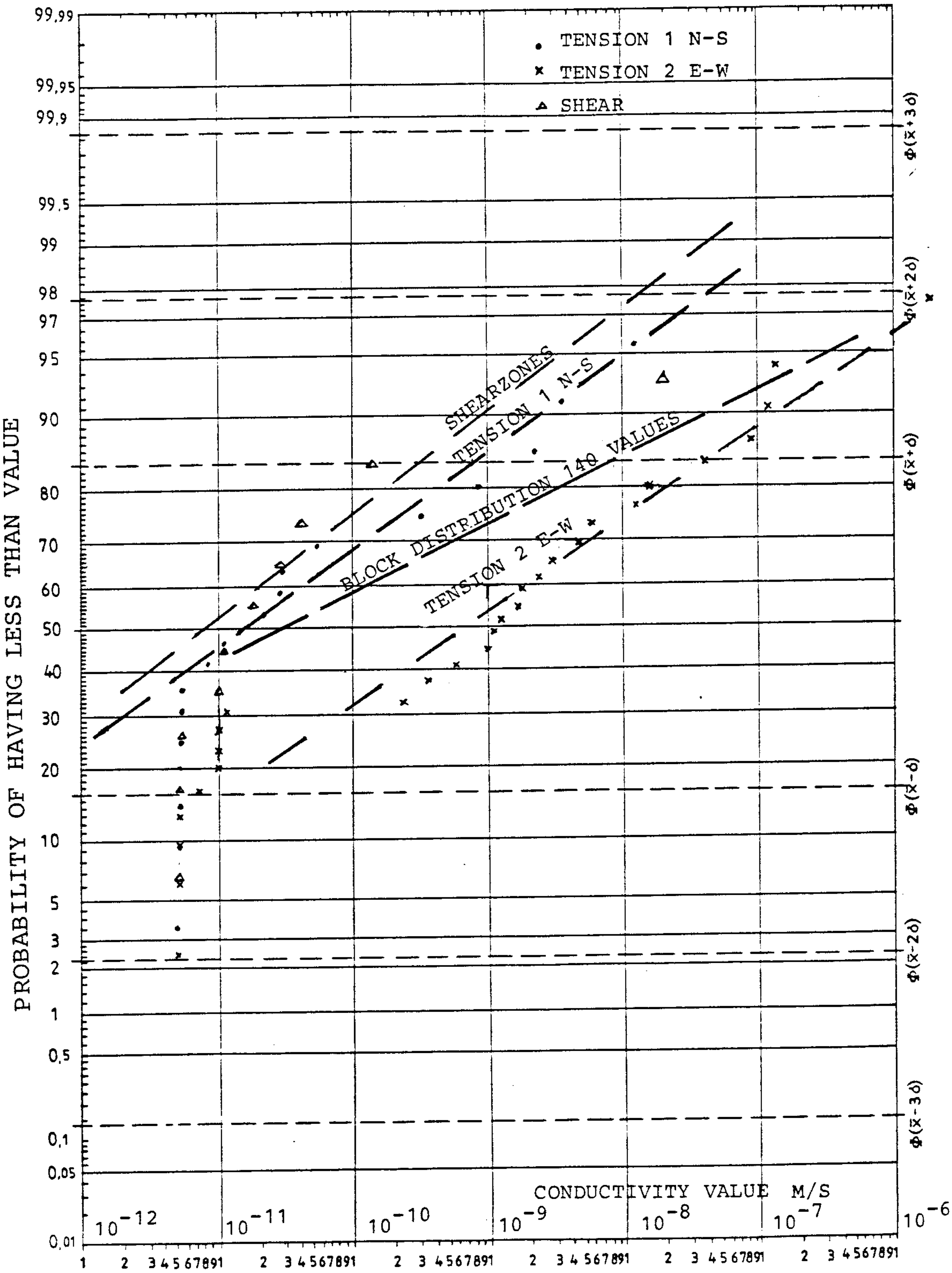

Figure 8.1 Plotted conductivity values at depths > 200 m. Adjusted lognormal distributions

The standard deviations of all the populations are unknown. In cases where the number of values don't exceed 30 the confidence intervals for the geometric means have been determined by using the t distribution.

From Table 8.1 it can be noticed that the largest deviation is found in the "Block sample". That is logic because of the heterogeneity of this tectonic element.

Regarding the tectonic condition, the East-Westerly fractures, sample Tension 2, show a mean value that is much higher than the other samples. The shearzones give the lowest sample mean value. The confidence intervals also confirm that the E-W tensional fractures generally seen have a higher conductivity compared to the N-S tensional fractures, the shear fractures and the undeformed parts of the blocks.

If one studies the fractures from 50 m below surface and downwards a statistical analysis still gives the same resulting trends. This confirms that the east-westerly tension fractures are the best water bearing zones.

In the previous chapter 7, specific capacity values from bedrock wells were analyzed. These values correspond to the conductivity down to about 150 m. Most of the wells are situated in migmatite and sedimentary gneiss. The geometric mean of the 63 "Block wells" was determined to 10,5 l/h,m. This value corresponds to a hydraulic conductivity of $K(p=0,5) \approx 2,7 \cdot 10^{-8}$ m/s (depth = 150 m).

Concerning the injection tests a statistical analysis of all 72 "Block values" from surface down to 200 m give $K(p=0,5) = 1,1 \cdot 10^{-8}$ m/s. Most of the tests have been carried out in migmatite. For the more shallow conductivity estimations there is in this case, in other words a rather good agreement between the mean values from the SGU well archives and the injection tests.

The hydraulic conductivity decreases versus depth for all studied samples. The decrease of values is not continuous. Because of the heterogenity there are great local variations. In figure 8.2 is for instance shown the mean conductivity of the three "Block" categories together with the depth intervals. The other samples have been fitted to an exponential function $K(z) = a \cdot e^{-bz}$ (See figure 8.3.) The regression curves are:

Tension fractures N-S $K = 1{,}2 \cdot 10^{-6} \cdot e^{-0{,}02 \cdot z}$; $R = -0{,}74$

Tension fractures E-W $K = 5{,}8 \cdot 10^{-8} \cdot e^{-0{,}007 \cdot z}$; $R = -0{,}38$

Shear fractures $K = 3{,}4 \cdot 10^{-9} \cdot e^{-0{,}009 \cdot z}$; $R = -0{,}63$

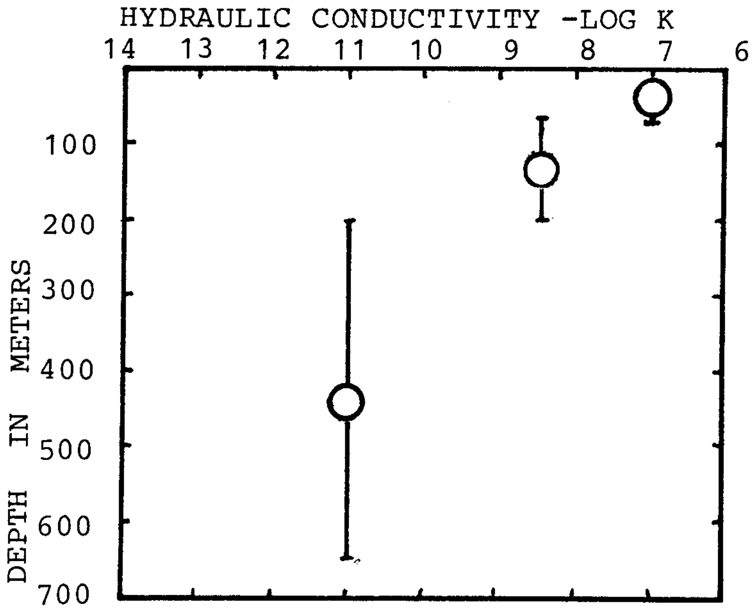

Figure 8.2 Mean conductivity versus depth for "Block" values

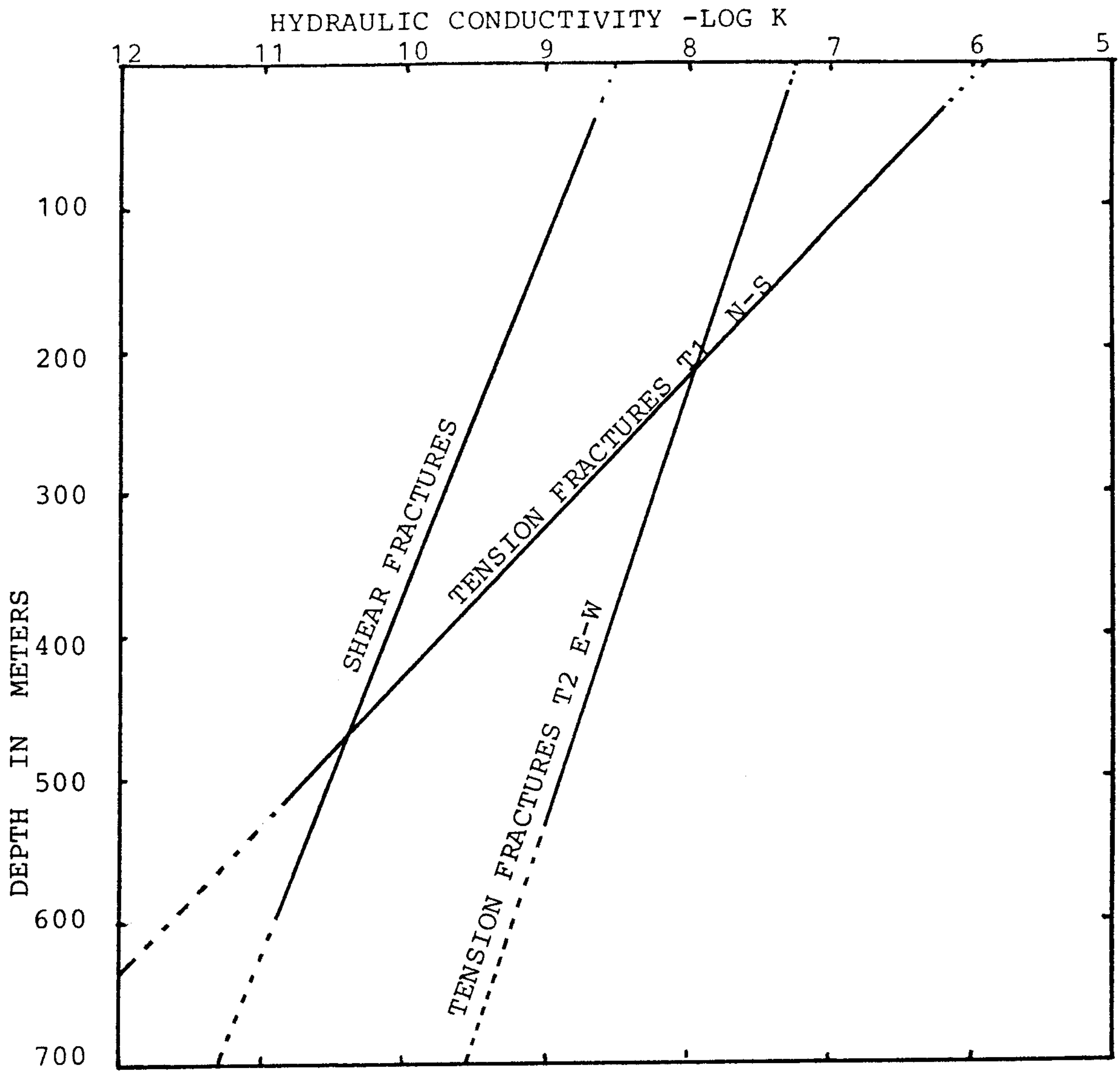

Figure 8.3 Regression curves of hydraulic conductivity versus depth for the two tensional sets and the shear fractures (See also equations on page 37)

9. CONCLUSIONS

A tectonic model within the Gideå site have been constructed based on a fracture mapping of the outcrops and by help of an interpretation of the topography and lineaments. The model has been refined by supplementary fracture measurements in the near Gissjö hydropower tunnel. Former geophysical investigations, slingram and magnetic anomalies, verify the model.

The following main directions have been found for the almost vertical fracture planes:

N-S	Tension T1
E-W	Tension T2
N30°E	Shear
N60°W	Shear

A lot of water injection tests have earlier been performed in core drilling holes within the Gideå site. The test data have been classified into tectonic elements. From a statistical point of view it has been found that the latest developed tension fractures, T2, in the east-westerly direction are outstanding concerning the waterbearing conditions. The mean conductivity value of the E-W tension fractures, at depths >200 m, is about 30-80 times higher than those of the undeformed parts of the blocks, the N-S tension fractures and the shearzones. (See figure 8.1.)

All samples generally show a decreasing conductivity versus depth. The N-S fractures reduce by approximately one conductivity decade per 100 m depth interval and the Blocks reduce little more than that. The E-W tension fractures and the shear zones reduce by about one third of a conductivity decade per 100 m. (See figure 8.2 and 8.3.)

The vital importance of the tension fractures regarding the permeability has also been verified by a statistical analysis of well data. The specific capacities of 163 wells at the SGU well archives have been statistically treated.

After evaluating the different fracture sets within the Gideå site it is evident that the most feasable directions of a tunnel system are N40^{o}W or N60^{o}E (see figure 4.3).

In order to further clarify the water leakage to a tunnel system and the inhomogenity in the bedrock one ought to carry out interference tests. By such a pumping test the elliptical form of the drawdown depression can be estimated more accurate and the main directions of underground constructions as well as a localization can be more proper designed.

REFERENCES

Ahlbom K, Carlsson L, Olsson O, 1983. Final disposal of spent nuclear fuel - geological, hydrogeological and geophysical methods for site characterization. SKBF/KBS Technical Report 83-43, Stockholm

Bolvede P, et al, 1983. Projektarbete Yxjöbergs Gruva, Geol. Inst CTH/GU, Göteborg

Carlsson L, Winberg A, Grundfelt B, 1983. Model calculations of the groundwater flow at Finnsjön, Fjällveden, Gideå and Kamlunge. SKBF/KBS Technical Report 83-45. Stockholm

Dagan G, 1979. Models of groundwater flow in statistically homogeneous formations. - Water Resources Research, Vol 15, No 1, Feb 1979, pp 47-63

Dagan G, 1981. Analysis of flow through Heterogeneous random aquifers by the method of embedding matrix. 1. Steady flow. - Water Resources Research, Vol 17, No 1, Feb 1981, pp 107-121

Ericsson L, Johansson I, 1984. Nacka kommun. Grundvattenstudie Boo, VIAK project 4912.03.8088. Stockholm

Freeze, R.A, 1975. A Stochastic-Conceptual Analysis of One-dimensional Groundwater Flow in Nonuniform Homogeneous Media. - Water Resources Research, Vol 11, No 5, Oct 1975, pp 725-741

Gustafson G, 1985. Geohydrologiska undersökningsmetoder i berg. Befo rapport (In print). Stockholm

Gustafson G, Liedholm M, 1984. Lyckeboprojektet. Utvärderingsprogram Geologi-Geohydrologi. Stiftelsen Bergteknisk forskning BeFo. Rapport 109:1/1984. Stockholm

Gustafson G, Liedholm, M, 1985. Vattenfall. Deep Gas Project. Hydraulic conductivity in the Siljan Ring Area. VIAK project 10.4.5412.42.1409. Gothenburg.

Gustafson G, Ronge B, 1981. Aitikgruvan geohydrologisk utredning - Boliden Mineral AB.

Gustafson G, Åberg B, 1985. Vattenfall-Deep Gas Project. Hydraulic Conditions in caprock and reservoir. VIAK project 5412.42.1409-01, Gothenburg, Rimbo

Lindberg E, et al, 1985. Hydrogeologiska undersökningar, Kirunagruvan nivå 795 m. Geol Inst CTH/GU, Göteborg

Lundgren L E, et al, 1985. Projektarbete Grängesbergs gruva. Geol Inst CTH/GU, Göteborg

Lundqvist T, 1979. The precambrian of Sweden, Swedish Geological Survey Publ, ser C, no 768, Uppsala

Nilsson K, Ronge B, 1985a. Nuvarande och framtida VA-försörjning, Aspö Karlskrona kommun. VIAK-project 850513. Malmö

Nilsson K, Ronge B, 1985b. Vattenförsörjning Brömsebro, Fågelmara, Karlskrona kommun. In press. VIAK-project. Malmö

VIAK, 1984. Eastern Botswana Regional Water Study. Main Report. Republic of Botswana. Ministry of Mineral Resources and Water Affaires, Department of Water Affaires. Stockholm

Warren, J.E, & Root, 1961: Flow in Heterogeneous Porous Media. Jour. Soc. of Pet. Eng. Sept 1961, pp153-169

APPENDIX 1

Wells within the topographic maps 19J NW, 19J NE, 20J SW and 20J SE registered at the well archives, SGU

EXPLANATION OF ABBREVIATIONS IN WELL DATA LISTS

FÖRS Code of administrative county, district and parish

FAST Real estate.

VMÄNGD Well yield in litres per hour. The yield is normally determined in a simple way (short pumping period, emptying by air-lift pumping or by floater). The pumping time is usually only one or some hours. Within the interval 0 - approx. 5 000 litres per hour the above mentioned methods are assumed to give a proper value of the well's momentary capacity. Differences from the true values can be considerable if the measured yield exceed approx. 5 000 litres per hour. In that case the momentary capacity usually is higher than the measured value.

JORDDJ Soil depth beneath ground surface. The value can be considered as relatively accurate. If there is a discrepancy compared to real conditions the listed value could be somewhat too high.

TOTDJ Total depth of well i metres. The information can be treated as accurate.

BA16 Code of general rock type (see attached data list).

BDAT Date of drilling (year, month, day).

ID Well number. The first four figures (TOP) state the code of topographic map in Sweden and the following running figures belong to the wells of each map.

EKON Figure code of economical map.

X,Y Coordinates.

VXY Classification of well position accurancy on map in theree classes (0, 1, 2).
0 means that the position on map differs less than 100 metres from the real position.
1 means that the position on map differs less than 250 metres from the real position.
2 means that the position on map is uncertain.

ROCK TYPE OF AQUIFER
====================

FD DOLORITE
HA REVSUNDS-FELLINGSBRO-STOCKHOLM GRANITE, YOUNG GRANITE
HC MIGMATITE
HF OLD GRANITE
HH SEDIMENTS, MAINLY GREYWACKES AND SCHISTS
HL SVIONIC LIMESTONE
HM SVIONIC GABBRO AND DIORITE
HX GENERAL SVIONIC ROCK TYPE

TECTONIC ELEMENT:	CODE
TENSION FRACTURES AND CROSS POINTS	1
SHEAR FRACTURES	2
BLOCKS	3

TOP	URNR	FORS	FAST	EDAT	VMÄNGD	JORDDJ	TOTDJ	BAIS	EKON	VXY	X	Y	Tect. element
1993	1	228402		59	700	0.	146.8	FD	19950	2	7029500	1653500	3
1993	2	228402		60	130	2.	87.7	FD	19950	2	7029500	1653500	3
1993	4	228410		60	1800	14.1	61.1	FD	19952	2	7027000	1660700	1
1993	5	228410		59	3450	1.6	55.1	HF	19953	2	7027500	1665000	3
1993	6	228410		06	25	0.	50.3	HC	19953	2	7029000	1668000	2
1993	7	228402		70	1000	0.	53.0	FD	19961	2	7031700	1657900	2
1993	8	228410		68	1500	1.7	78.0	HF	19962	2	7032500	1664600	3
1993	10	228410		61	720	1.	119.0	HF	19963	2	7032700	1668700	3
1993	11	228410		65	300	0.	36.8	HC	19964	2	7031500	1670800	3
1993	12	228410		65	1800	0.	40.4	HC	19963	2	7032000	1669500	2
1993	13	228410		65	1200	3.6	27.4	HC	19963	2	7032000	1669500	2
1993	14	228410		65	140	3.7	28.7	HC	19963	2	7032000	1669500	2
1993	15	228410		68	1200	5.	31.0	HC	19963	2	7032000	1669500	2
1993	16	228410		65	900	3.6	35.9	HC	19964	2	7030400	1670800	2
1993	17	228410		65	225	1.9	92.6	HC	19964	2	7030400	1670800	2
1993	18	228410		70	450	1.5	75.0	HC	19964	2	7030400	1670800	2
1993	19	228410		69	385	1.	90.0	HC	19972	2	7036800	1662500	3
1993	20	228402		69	370	1.	35.0	HC	19972	2	7036500	1662000	2
1993	21	228402		60	800	7.	100.3	HC	19972	2	7036500	1662000	2
1993	22	228410		69	1500	0.	71.0	HF	19973	2	7035600	1669900	3
1993	23	228411		69	0	6.4	103.0	HC	19982	2	7041000	1663200	-
1993	24	228411		70	1800	2.5	100.0	HC	19982	2	7041000	1663200	1
1993	25	228411		70	2400	5.	75.0	HC	19982	2	7041000	1663200	1
1993	26	228410		67	2000	1.5	74.0	HC	19984	2	7043200	1672200	3
1993	27	228410		68	....	0.	104.0	HC	19993	2	7046400	1668800	-
1993	28	228410		70	400	3.	63.	HC	19993	2	7046400	1668800	1
1993	29	228410		67	1800	1.5	52.2	HF	19952	2	7026600	1664200	1
1993	30	240102	AVA 1:15	770608	1000	2.	40.	HC	19994	2	7046200	1674300	3
1993	31	228410	ÖSTERSTENSÄTER 1:18	770614	50	3.	100.	HF	19953	0	7025640	1666340	3
1993	32	228402	BRUNNSNYLAND 3:11	770406	75	3.	80.	FD	19950	0	7029980	1652130	2
1993	33	228410	DOMBÄCKSMARK 1:5	770202	1500	9.	55.	HF	19962	0	7032360	1664700	1
1993	35	228411	SÖRGIDSJÖ 2:16	770309	750	12.	61.	HA	19981	0	7044710	1656970	3
1993	36	228410	SALUBÖLE 1:9	771205	800	34.	100.	HC	19984	0	7044380	1672000	2
1993	37	240102	STORSANDEN AV 13:1	810209	1250	14.	110.	HC	19994	0	7045050	1673450	2
1994	1	240107		61	450	0.	48.0	FD	19988	2	7043300	1692800	3
1994	2	240102		68	1800	13.5	62.0	FD	19988	2	7043300	1692800	3
1994	3	240102		70	400	18.5	64.0	FD	19988	2	7043300	1692800	3
1994	4	240102		70	90	8.	90.0	FD	19988	2	7043300	1692800	3
1994	5	240102		70	175	10.	98.0	FD	19988	2	7043300	1692800	3
1994	6	240102		70	1000	12.	80.0	FD	19988	2	7043300	1692800	3
1994	7	240102		70	....	11.	38.0	FD	19988	2	7043300	1692800	-
1994	8	240102		65	....	0.	61.0	FD	19988	2	7043300	1692800	-
1994	9	240102		63	675	1.8	40.0	FD	19988	2	7042100	1693000	3
1994	10	240102	ÖRESUND 1:27	770607	550	3.	80.	HC	19986	2	7042300	1682600	3
1994	11	240102	ÖRESUND 2:2	760804	20	3.	100.	HC	19986	2	7042300	1682600	3
1994	13	240102	RÖNHOLM 6:1	760825	25	12.	100.	HC	19995	2	7049000	1678700	3
1994	14	240102	RÖNNHOLM 6:1	760405	1200	3.	60.	HC	19995	2	7049000	1678700	3
1994	15	240102	JÄRNÄS 5:78	770601	5000	3.	40.	HC	19998	2	7046600	1691200	2
1994	16	240102	JÄRNÄS 1:25	760824	500	9.	58.	HC	19998	2	7046600	1691200	2
1994	17	240102	JÄRNÄS 1:25	760820	15	6.	100.	HC	19998	2	7046600	1691200	2
1994	18	240102	JÄRNÄS 4:5	760816	2000	21.	60.	HC	19998	2	7046600	1691200	2
1994	19	240102	JÄRNÄS 2:2	761108	300	6.	50.	HC	19998	2	7046600	1691200	2
1994	20	240102	JÄRNÄS 1:74	761203	1000	3.	40.	HC	19998	2	7046600	1691200	2
1994	21	240102	JÄRNÄS 6:16	761208	700	6.	82.	HC	19998	2	7046600	1691200	2
1994	22	240102	KRÅKEN 6:37	761207	1000	5.	87.	HC	19999	2	7048900	1696300	1
1994	23	240102	ANKRIKREVET	770602	2000	3.	50.	HC	19999	2	7048900	1696300	1
1994	24	240102			100	6.	150.	FD	19988	2	7042000	1691800	2
1994	24	240102			300	6.	150.	FD	19988	2	7042000	1691800	-
1994	25	240102	AVA 5:33	800211	2000	1.	90.	HC	19985	0	7043800	1675950	3
1994	26	240102	AVA 5:27	800130	500	1.	37.	HC	19985	0	7043200	1675900	3

TOP	ERNR	FÖRS	FAST	BDAT	VMÄNGD	JORDDJ	TOTDJ	BA16	EKON	VXY	X	Y	Tect. element
1994	27	240102	AVA 5:4	780426	500	6.	103.	HC	19995	0	7047880	1678520	2
1994	28	240102	AVA 5:39	780310	1000	1.5	100.	HC	19995	0	7047700	1678650	2
1994	29	240102	GA RONNHOLM 1:9	781023	2400	4.	88.	HC	19995	2	7049100	1678730	3
1994	30	240101	JÄRNÄS 1:32	801029	450	5.5	60.	HC	19988	0	7043200	1692500	3
1994	31	240102	JÄRNÄS 19:3	810429	750	0.	47.	FD	19988	0	7043650	1694500	1
1994	32	240102	JÄRNÄS 4:13	810427	400	1.	79.	HC	19998	2	7048600	1690050	3
1994	33	240102	JÄRNÄS 3:18	810527	1000	1.5	70.	HC	19998	0	7046680	1691150	2
1994	34	240102	JÄRNÄS 1:60	810202	1250	5.	100.	HC	19998	0	7042850	1691550	3
2091	1	228413		68	425	3.0	90.0	HC	20930	2	7068700	1651200	3
2091	2	228411		67	120	3.5	64.4	HA	20911	2	7059000	1656500	3
2091	3	228411		70	500	5.0	100.0	HC	20912	2	7055900	1660400	2
2091	5	228413		510125	10500	12.3	93.9	HC	20930	2	7068700	1651200	3
2091	6	240101		68	1350	8.5	85.0	HA	20934	2	7066100	1673100	3
2091	7	240101	STAVSJÖHOLM 1:20 NORDLUND	761123	1000	9.	40.	HA	20934	2	7066100	1673100	3
2091	8	240102	ORRBÖLE NR 2	760914	400	18.	63.	HC	20944	2	7073000	1673500	1
2091	9	228411	GRÖSSJÖ FLÄRKE 4:90	770927	324	6.	100.	HF	20912	0	7057160	1663290	3
2091	10	228411	FLÄRKE 4:51	770308	......	6.	61.	HH	20913	0	7057500	1667340	-
2091	11	228411	FLÄRKE 4:66	770303	600	15.	52.	HC	20912	0	7056050	1661040	1
2091	12	228411	LÅNGVIKEN 1:42	761011	1500	14.	84.	HH	20932	0	7066260	1661690	2
2091	13	228413	LEMESJÖ 1:107	770729	300	12.	40.	HH	20931	0	7066810	1657640	3
2091	14	228413	KARLSVIKEN 1:74	770804	500	32.	79.	HF	20930	1	7068830	1652170	3
2091	17	240102	ORRBÖLE 2:35	780504	300	1.5	120.	HC	20944	0	7074300	1672550	2
2091	18	240101	ORRBÖLE 1:8	780217	350	2.	43.	HA	20944	0	7074820	1671530	1
2091	19	240102	NORDSJÖ 1:68	781018	700	2.	94.	HC	20942	0	7073800	1660500	3
2091	20	240102	ORRBÖLE 1:3	780404	1200	0.	43.	HA	20944	2	7074750	1671000	1
2091	21	240102	ORRBÖLE 2:39	780428	200		40.	HC	20944	0	7074200	1672540	2
2091	22	240102	BERGSJÖ 1:9 1:18	780131	1200	0.	40.	HC	20923	0	7064580	1666360	1
2091	23	240102	VÄSTANSJÖ 1:7	780728	70	4.	100.	HC	20941	0	7073990	1656370	2
2091	24	240102	BERGSJÖ 1:28	780202	1400	6.	40.	HC	20923	0	7063550	1667530	3
2092	1	240102	BREDVIK 6:14 6:19	760827	150	9.	75.	HC	20907	2	7053300	1688750	2
2092	2	240102	BAGGÅRD 6:1	771220	350	6.	82.	HM	20925	2	7064300	1679000	2
2092	3	240102		61	720	4.	50.	HA	20906	2	7052700	1681300	3
2092	4	240102		58	4140	14.0	42.0	HC	20916	2	7056800	1684800	1
2092	5	240102		70	2400	9.0	63.0	HC	20918	2	7055500	1693100	1
2092	6	240102		69	3200	20.5	76.0	HC	20918	2	7055500	1693100	1
2092	7	248007		70	480	13.0	90.0	HC	20919	1	7055000	1696000	1
2092	8	248007		73	1500	0.	53.3	HC	20919	2	7057000	1699600	1
2092	9	248007		67	450	9.0	67.0	HC	20919	2	7057000	1699600	1
2092	10	240102		64	900	4.6	35.4	HA	20925	2	7063700	1677300	3
2092	11	240102		68	1000		100.0	HA	20925	2	7063700	1677300	3
2092	12	240102		68	1800	11.0	50.0	HL	20925	2	7064200	1679000	3
2092	13	240102		66	600	5.5	70.0	HC	20928	2	7060900	1691800	3
2092	14	240102		66	3600	15.0	38.1	HC	20928	2	7060900	1691800	3
2092	15	240102		72	100	4.5	90.0	HC	20937	1	7067600	1689600	3
2092	16	240102		72	100	10.0	110.0	HC	20937	2	7067600	1689600	3
2092	17	248007		68	0	0.	90.0	HC	20949	2	7072080	1698300	-
2092	18	240102		36	90	3.6	24.1	HA	20906	1	7052700	1681300	3
2092	19	240102		35	900	0.	20.9	HA	20906	1	7052700	1681300	3
2092	20	240102		35	200	4.	17.	HA	20906	1	7052700	1681300	3
2092	21	240102		35	1400	0.	47.	HA	20906	2	7053000	1680700	1
2092	22	240102		35	450	0.	11.9	HA	20906	2	7053000	1680700	1
2092	23	240102		37	5700	6.3	40.	HC	20916	2	7056800	1683400	1
2092	24	240102		37	3600	5.	35.	HC	20916	2	7056800	1683400	1
2092	25	240102		37	5400		62.5	HC	20916	2	7056800	1683400	1
2092	26	240102		38	12000	3.	43.	HC	20916	2	7056000	1683400	2
2092	27	240102		47	7200	5.5	71.5	HC	20916	2	7056800	1683400	1
2092	28	240102		46	17000	1.4	51.4	HC	20916	2	7056800	1683400	1
2092	29	240102		531114	5500	1.8	107.8	HC	20916	2	7056800	1683400	1
2092	30	240102		46	6500	0.	33.8	HC	20916	2	7056800	1684800	1
2092	31	240102		47	5300		[illegible]	HC	20916	2	[illegible]	[illegible]	[illegible]

TOP	BRNR	FÖRS	FAST	PDAT	VMANGD	JORDDJ	TOTDJ	BA16	EKON	VKY	X	Y	Tect. element
2092	32	240102		46	3000	10.1	52.6	HC	20916	2	7056800	1684800	1
2092	33	240102		501107	1200	12.0	55.0	HC	20916	2	7056800	1684800	1
2092	34	240102		500830	4800				20916	2	7056800	1684800	-
2092	34	240102		500830	4800			HC	20916	2	7056800	1684800	-
2092	35	240102		48	5500	1.9	56.0	HC	20916	2	7057800	1680700	3
2092	36	240102		39	3000	20.5	90.0	HC	20918	1	7056500	1693700	1
2092	37	248007		36	120	6.4	23.8	HC	20919	2	7057000	1699600	1
2092	38	248007		45	5500	1.0	31.3	HC	20919	2	7057000	1699600	1
2092	39	248007		46	1000	7.4	46.1	HC	20919	2	7057000	1699600	1
2092	40	248007		46	900	2.5	13.5	HC	20919	2	7057000	1699600	1
2092	41	248007		46	225	2.5	35.0	HC	20919	2	7057000	1699600	1
2092	42	248007		68	0	0.	90.0	HC	20949	2	7072280	1698050	-
2092	43	240102	LÖGDEÅ 8:51	770913	0	1.	115.	HA	20905	2	7053800	1678200	-
2092	44	248007	NORRBYN 1:85	770712	8000	4.	150.	HC	20919	2	7056900	1699600	1
2092	45	240102	BAGGÅRD 2:18	760413	900	3.	68.	HM	20925	2	7063700	1677300	3
2092	46	240102	BAGGÅRD 1:21	760406	720	3.	58.	HM	20925	2	7063700	1677300	3
2092	47	240102	BAGGÅRD 1:27	760926	750	15.	91.	HM	20925	2	7063700	1677300	3
2092	48	240102	LEDUSJÖ 4:1	760408	500	12.	100.	HM	20925	2	7063300	1679100	3
2092	49	240101	LÅNGED NR 5 P FORSBERG	761119	1500	15.	58.	HC	20928	2	7060800	1691800	3
2092	50	240102	LÅNGED 9:1	760405	2000	24.	82.	HC	20928	2	7060800	1691800	3
2092	51	240102	FJUPSJÖ 3:36	760503	200	6.	100.	HC	20935	2	7068200	1679700	2
2092	52	240102	DJUPSJÖ 5:1	760503	700	12.	100.	HC	20935	2	7068200	1679700	2
2092	53	240102	DJUPSJÖ 1:14	760428	600	12.	112.	HC	20935	2	7068200	1679700	2
2092	54	240101	DJUPSJÖ 2:22	761129	600	3.	61.	HC	20935	2	7068200	1679700	2
2092	55	240102	LEVAR 3:18	780209	1000		73.	HC	20907	1	7052580	1686530	2
2092	56	240102	HÄKNÄS 5:34	781002	2000	4.	63.	HC	20909	0	7054610	1697320	1
2092	57	240102	DJUPSJÖ 2:21	780313	2000	0.	47.	HC	20935	0	7067390	1679730	3
2092	59	240102	BAGGÅRD 2:18	781006	700	2.	100.	HC	20925	0	7064660	1678730	3
2092	62	248007	ÄNGERSJÖ	781205	2000	0.	53.	HA	20929	2	7063650	1697350	1
2092	63	248007	SÖRBYN 7:1	780502	3000	12.	55.	HC	20919	0	7055050	1696020	1
2092	64	240102	LEDUSJÖ 1:9	800217	53640	13.	13.		20925	2	7063300	1679150	-
2092	65	240102	SUNNANSJÖ 2:19	800410	2500	4.	40.	HA	20925	0	7063730	1677220	3
2092	66	240101	SUNNANSJÖ 1:43	801024	520	8.8	100.	HA	20925	0	7064080	1677450	1
2092	67	248007	NORRBYN 1:34	810312	500	2.5	55.	HC	20919	1	7056850	1699400	1
2092	68	240101	BAGGÅRD 1:19	801028	1735	2.5	52.	HX	20925	2	7064300	1679050	3

155 ROW(S) FOUND

APPENDIX 2

Plotted distribution of Specific capacity

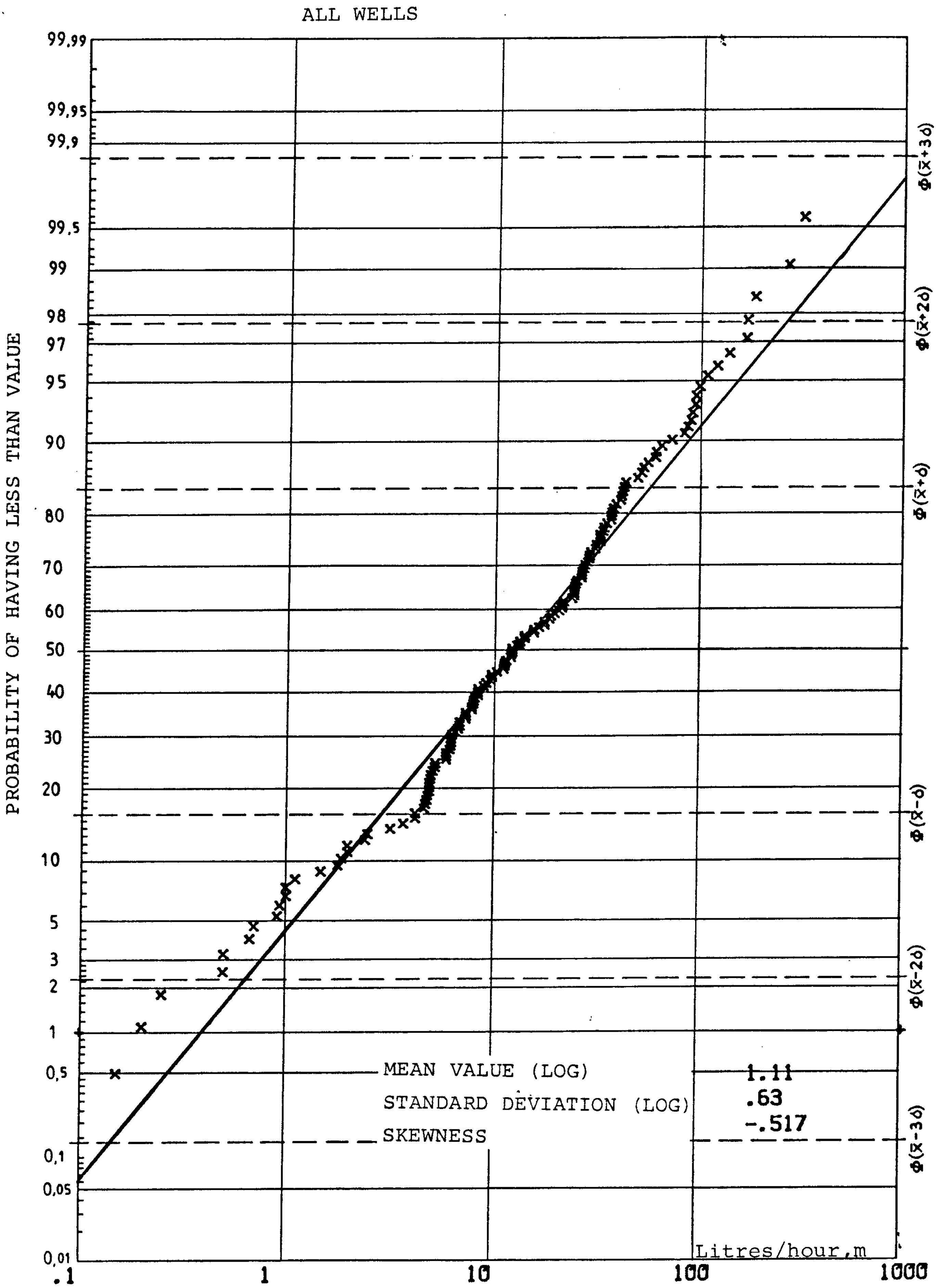
ALL WELLS
PROBABILITY OF HAVING LESS THAN VALUE
99,99
99,95
99,9
99,5
99
98
97
95
90
80
70
60
50
40
30
20
10
5
3
2
1
0,5
0,1
0,05
0,01
Φ(x̄+3σ)
Φ(x̄+2σ)
Φ(x̄+σ)
Φ(x̄-σ)
Φ(x̄-2σ)
Φ(x̄-3σ)
MEAN VALUE (LOG) 1.11
STANDARD DEVIATION (LOG) .63
SKEWNESS -.517
Litres/hour,m
.1
1
10
100
1000

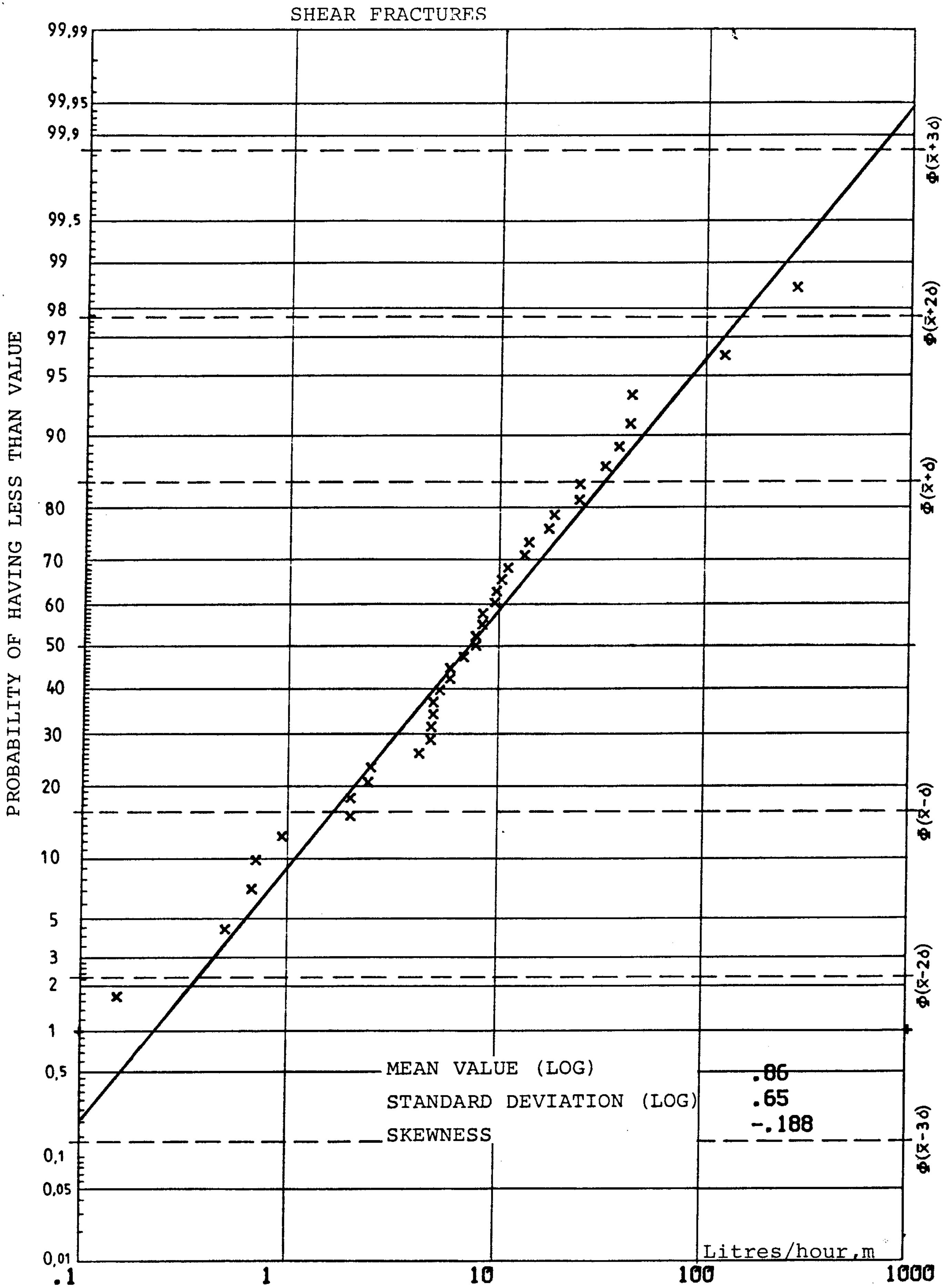
SHEAR FRACTURES
PROBABILITY OF HAVING LESS THAN VALUE
99,99
99,95
99,9
99,5
99
98
97
95
90
80
70
60
50
40
30
20
10
5
3
2
1
0,5
0,1
0,05
0,01
.1
1
10
100
1000
Litres/hour,m
MEAN VALUE (LOG) .86
STANDARD DEVIATION (LOG) .65
SKEWNESS -.188
Φ(x̄+3σ)
Φ(x̄+2σ)
Φ(x̄+σ)
Φ(x̄-σ)
Φ(x̄-2σ)
Φ(x̄-3σ)

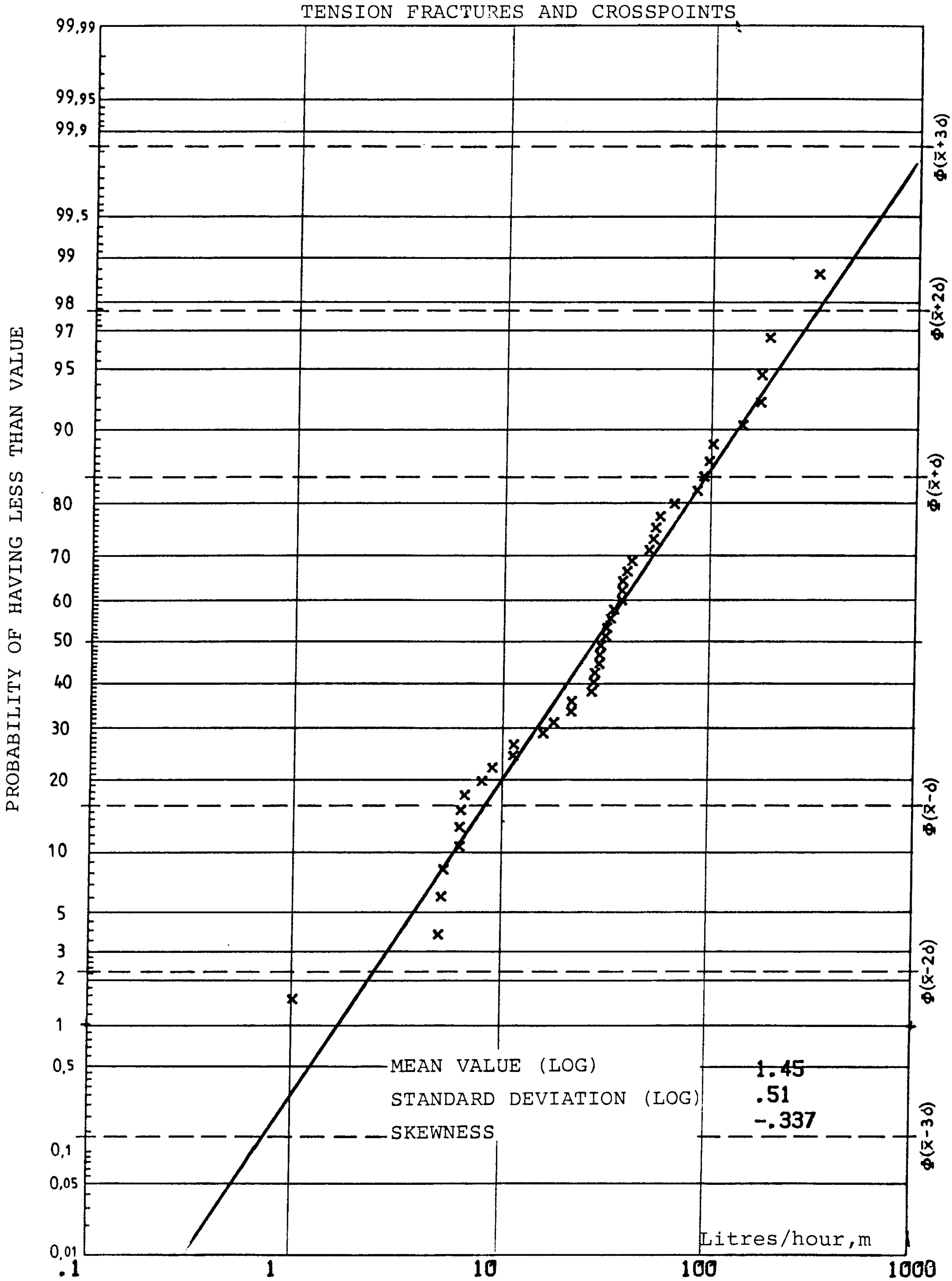
TENSION FRACTURES AND CROSSPOINTS
PROBABILITY OF HAVING LESS THAN VALUE
99,99
99,95
99,9
99,5
99
98
97
95
90
80
70
60
50
40
30
20
10
5
3
2
1
0,5
0,1
0,05
0,01
$\Phi(\bar{x}+3\sigma)$
$\Phi(\bar{x}+2\sigma)$
$\Phi(\bar{x}+\sigma)$
$\Phi(\bar{x}-\sigma)$
$\Phi(\bar{x}-2\sigma)$
$\Phi(\bar{x}-3\sigma)$
MEAN VALUE (LOG) 1.45
STANDARD DEVIATION (LOG) .51
SKEWNESS -.337
Litres/hour,m
.1
1
10
100
1000

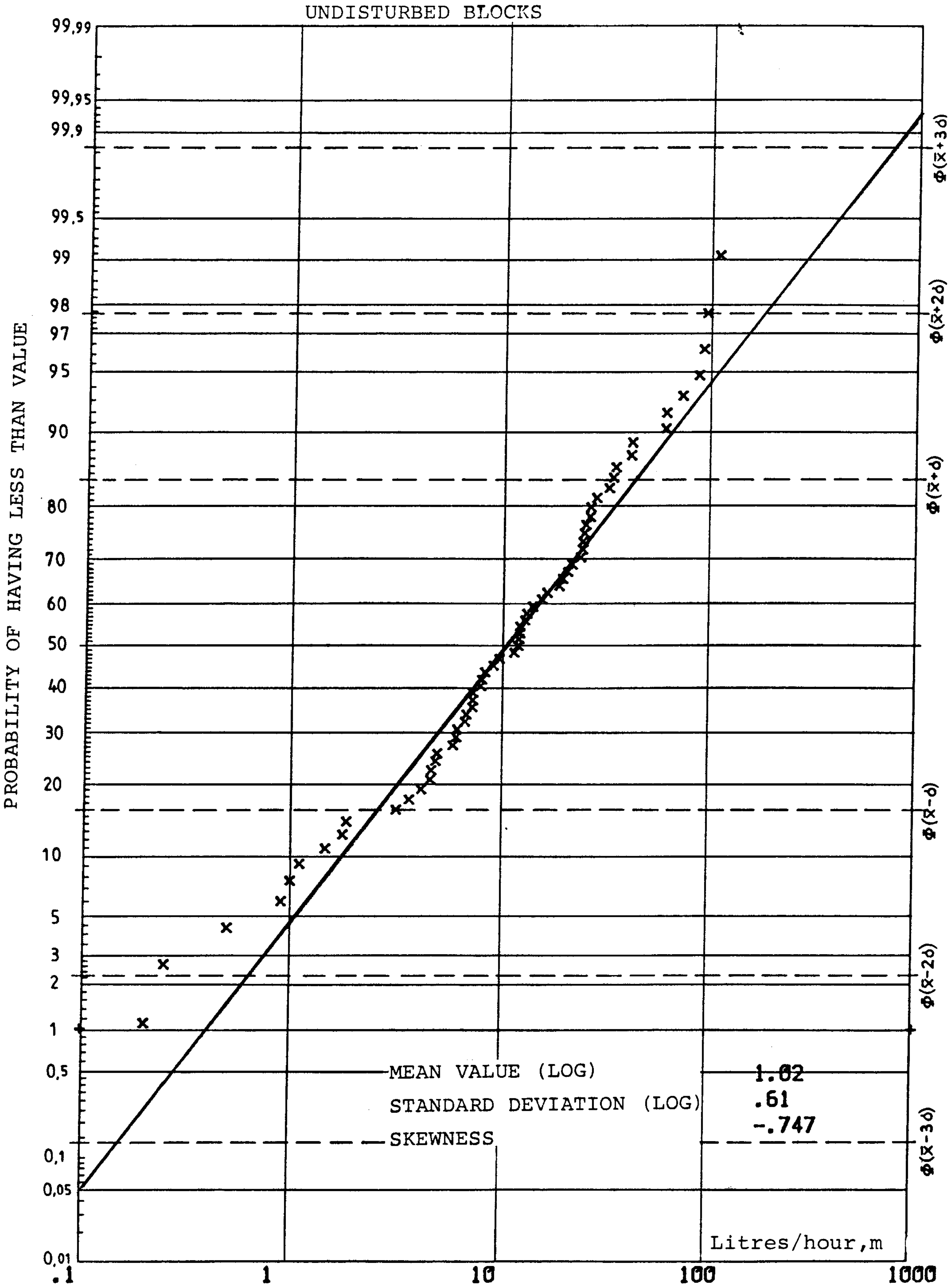
UNDISTURBED BLOCKS
PROBABILITY OF HAVING LESS THAN VALUE
99,99
99,95
99,9
99,5
99
98
97
95
90
80
70
60
50
40
30
20
10
5
3
2
1
0,5
0,1
0,05
0,01
.1
1
10
100
1000
Litres/hour,m
MEAN VALUE (LOG)
STANDARD DEVIATION (LOG)
SKEWNESS
1.02
.61
-.747
$\Phi(\bar{x}+3\delta)$
$\Phi(\bar{x}+2\delta)$
$\Phi(\bar{x}+\delta)$
$\Phi(\bar{x}-\delta)$
$\Phi(\bar{x}-2\delta)$
$\Phi(\bar{x}-3\delta)$

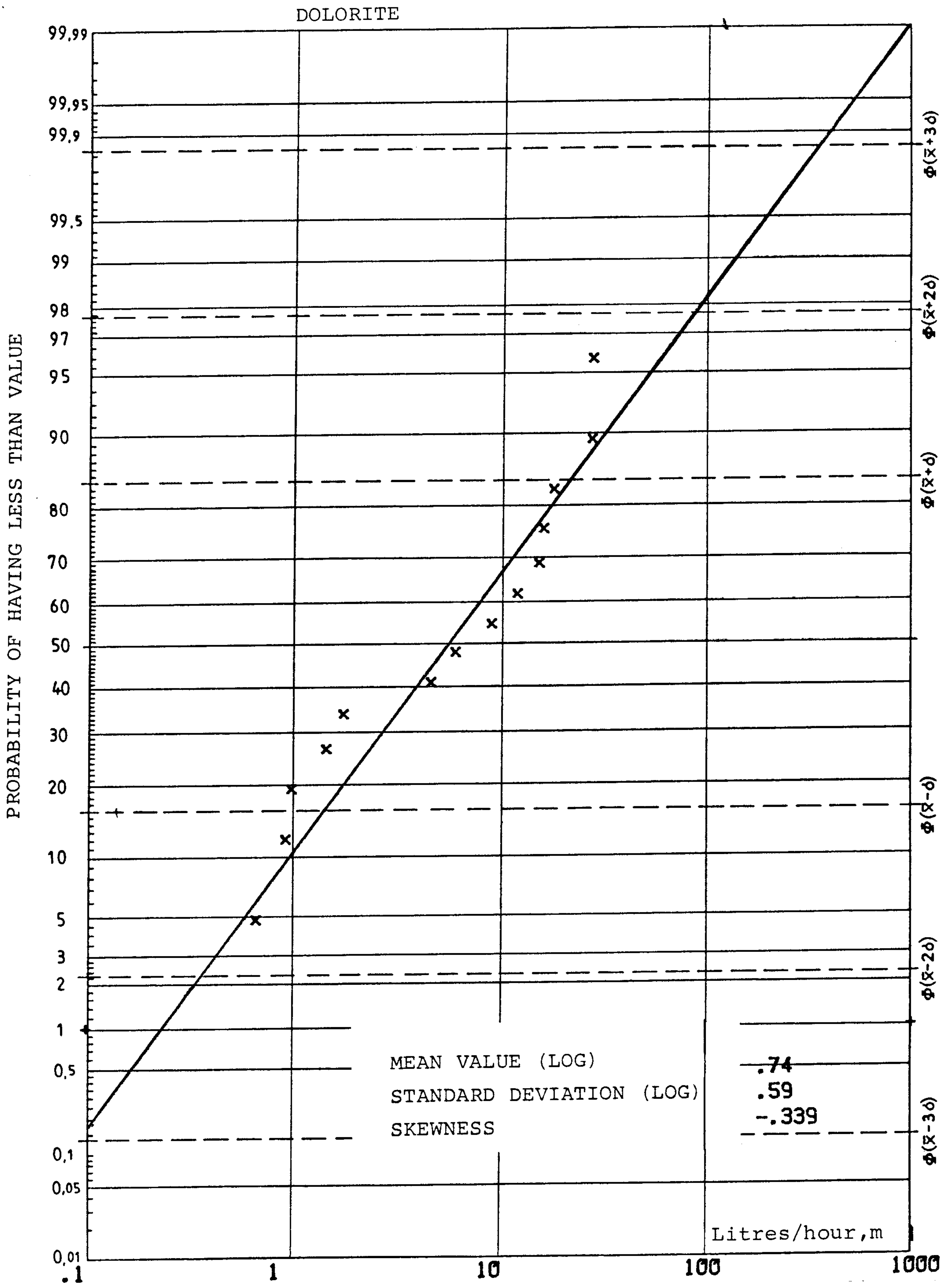
DOLORITE
PROBABILITY OF HAVING LESS THAN VALUE
99,99
99,95
99,9
99,5
99
98
97
95
90
80
70
60
50
40
30
20
10
5
3
2
1
0,5
0,1
0,05
0,01
.1
1
10
100
1000
Litres/hour,m
Φ(x̄+3σ)
Φ(x̄+2σ)
Φ(x̄+σ)
Φ(x̄-σ)
Φ(x̄-2σ)
Φ(x̄-3σ)
MEAN VALUE (LOG)
STANDARD DEVIATION (LOG)
SKEWNESS
.74
.59
-.339

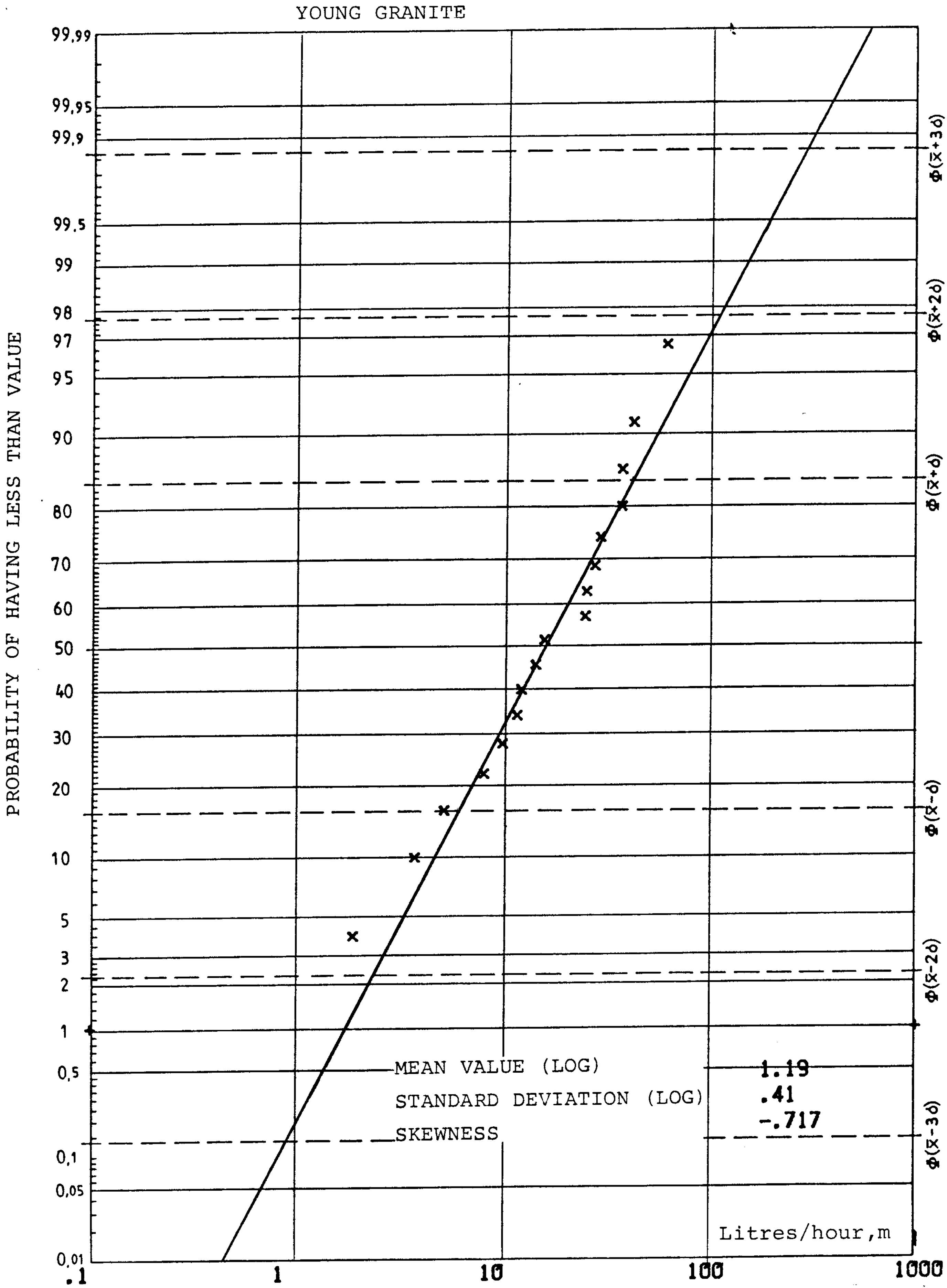
YOUNG GRANITE
PROBABILITY OF HAVING LESS THAN VALUE
99,99
99,95
99,9
99,5
99
98
97
95
90
80
70
60
50
40
30
20
10
5
3
2
1
0,5
0,1
0,05
0,01
Φ(x̄+3σ)
Φ(x̄+2σ)
Φ(x̄+σ)
Φ(x̄-σ)
Φ(x̄-2σ)
Φ(x̄-3σ)
MEAN VALUE (LOG) 1.19
STANDARD DEVIATION (LOG) .41
SKEWNESS -.717
Litres/hour,m
.1
1
10
100
1000

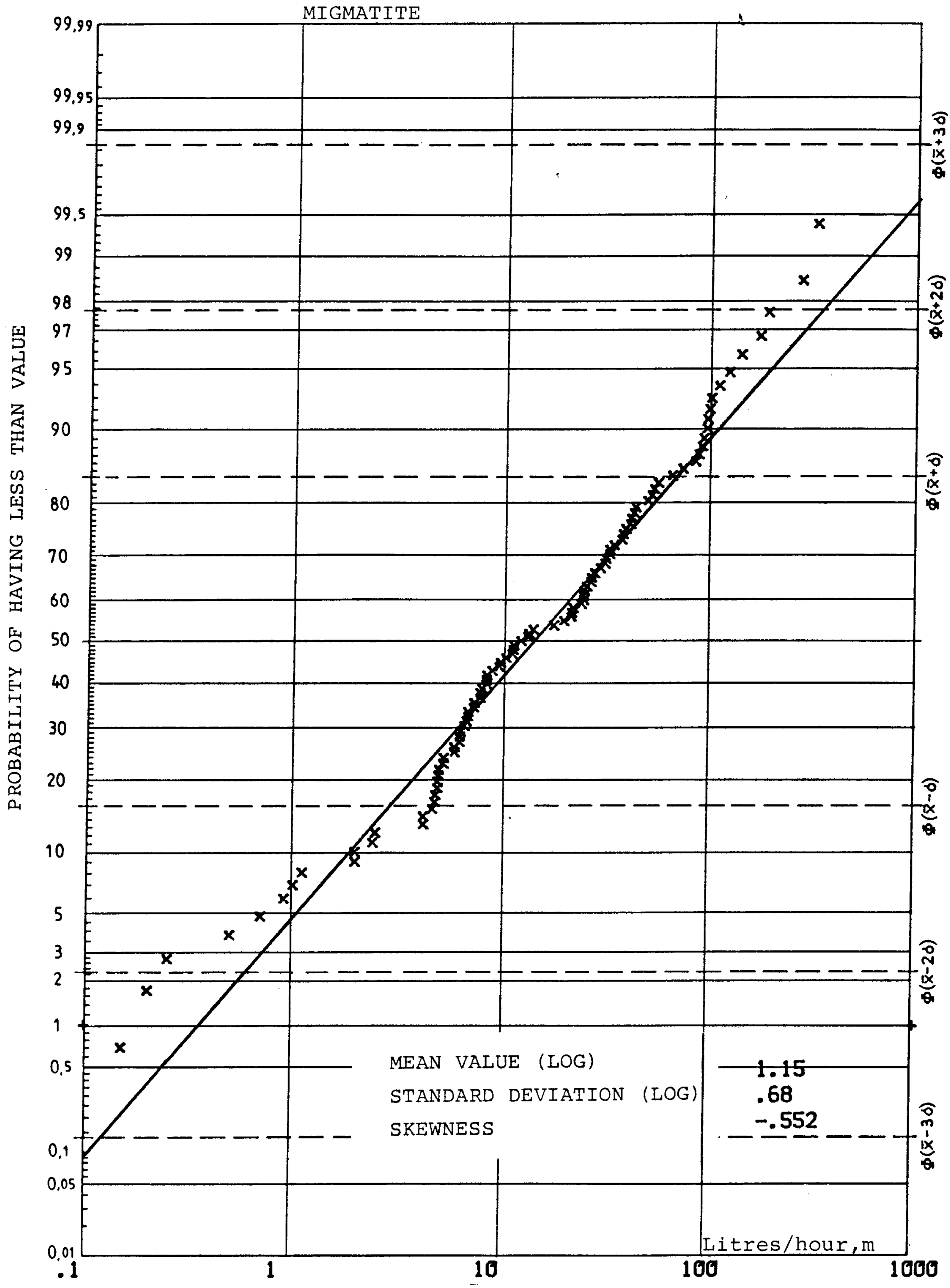

MIGMATITE
PROBABILITY OF HAVING LESS THAN VALUE
99,99
99,95
99,9
99,5
99
98
97
95
90
80
70
60
50
40
30
20
10
5
3
2
1
0,5
0,1
0,05
0,01
Φ(x̄+3σ)
Φ(x̄+2σ)
Φ(x̄+σ)
Φ(x̄-σ)
Φ(x̄-2σ)
Φ(x̄-3σ)
MEAN VALUE (LOG) 1.15
STANDARD DEVIATION (LOG) .68
SKEWNESS -.552
Litres/hour,m
.1
1
10
100
1000

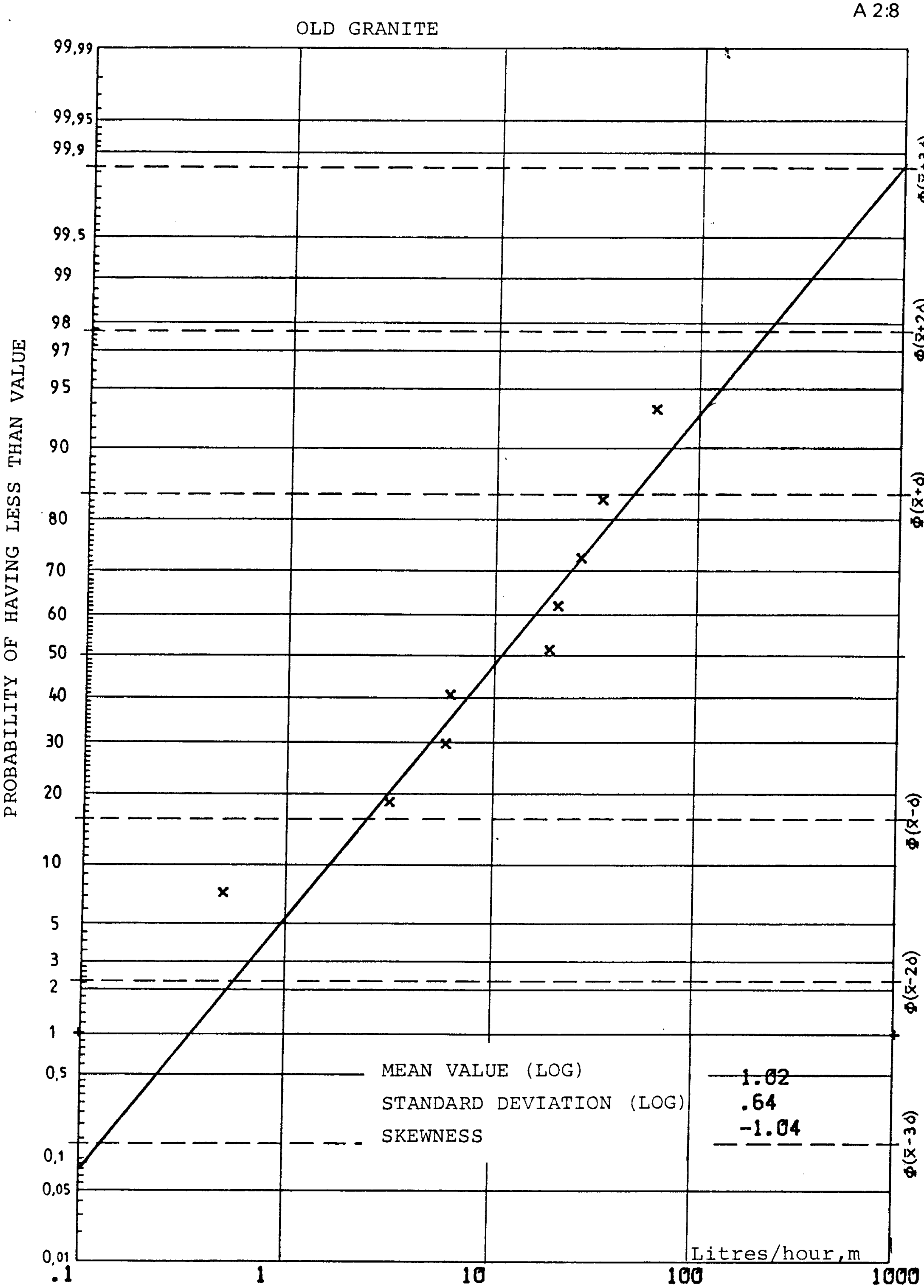

OLD GRANITE
PROBABILITY OF HAVING LESS THAN VALUE
99,99
99,95
99,9
99,5
99
98
97
95
90
80
70
60
50
40
30
20
10
5
3
2
1
0,5
0,1
0,05
0,01
.1
1
10
100
1000
Litres/hour,m
MEAN VALUE (LOG) 1.02
STANDARD DEVIATION (LOG) .64
SKEWNESS -1.04
Φ(x̄+3σ)
Φ(x̄+2σ)
Φ(x̄+σ)
Φ(x̄-σ)
Φ(x̄-2σ)
Φ(x̄-3σ)

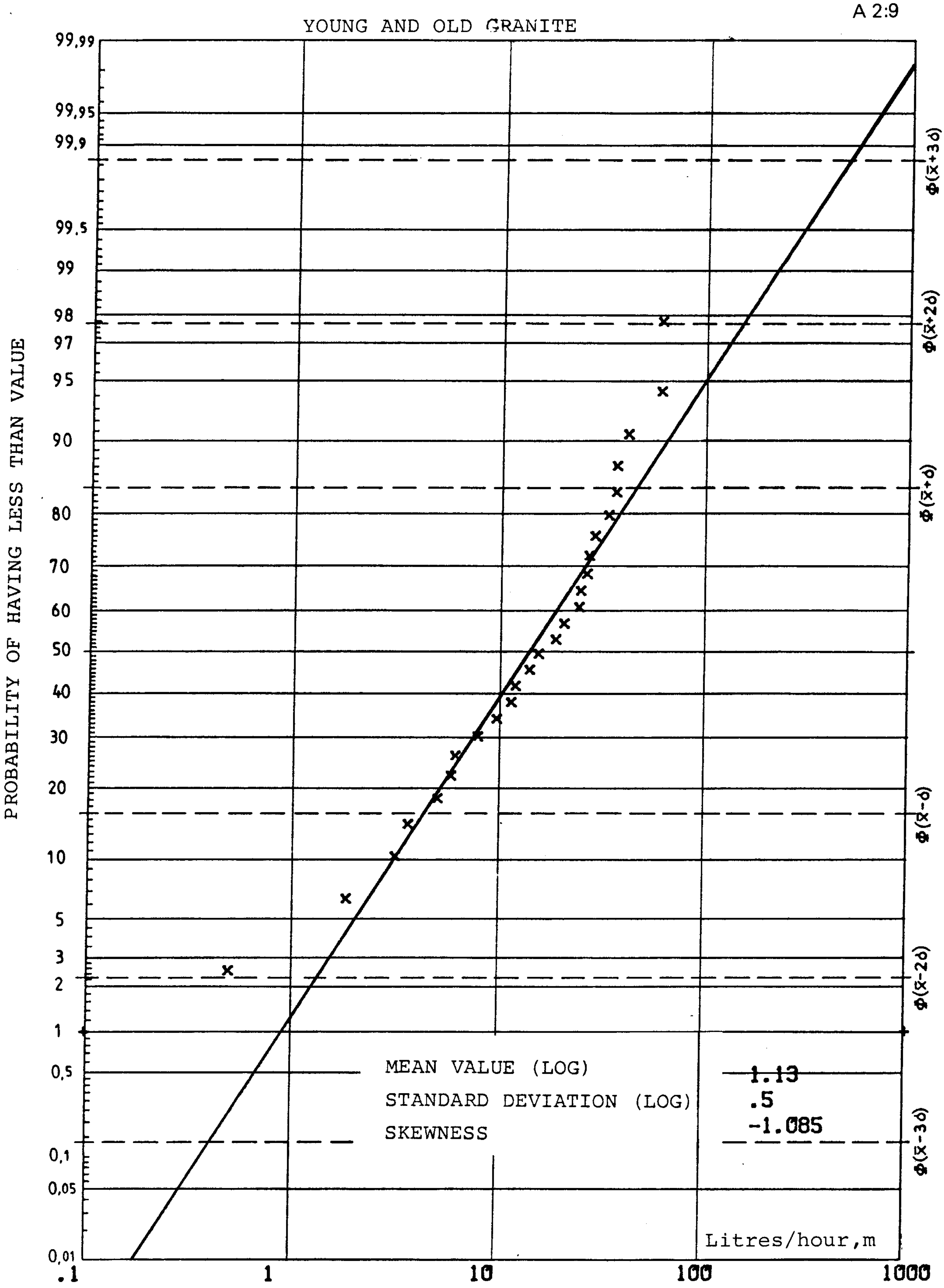
YOUNG AND OLD GRANITE
PROBABILITY OF HAVING LESS THAN VALUE
99,99
99,95
99,9
99,5
99
98
97
95
90
80
70
60
50
40
30
20
10
5
3
2
1
0,5
0,1
0,05
0,01
.1
1
10
100
1000
Litres/hour,m
Φ(x̄+3σ)
Φ(x̄+2σ)
Φ(x̄+σ)
Φ(x̄-σ)
Φ(x̄-2σ)
Φ(x̄-3σ)
MEAN VALUE (LOG) 1.13
STANDARD DEVIATION (LOG) .5
SKEWNESS -1.085

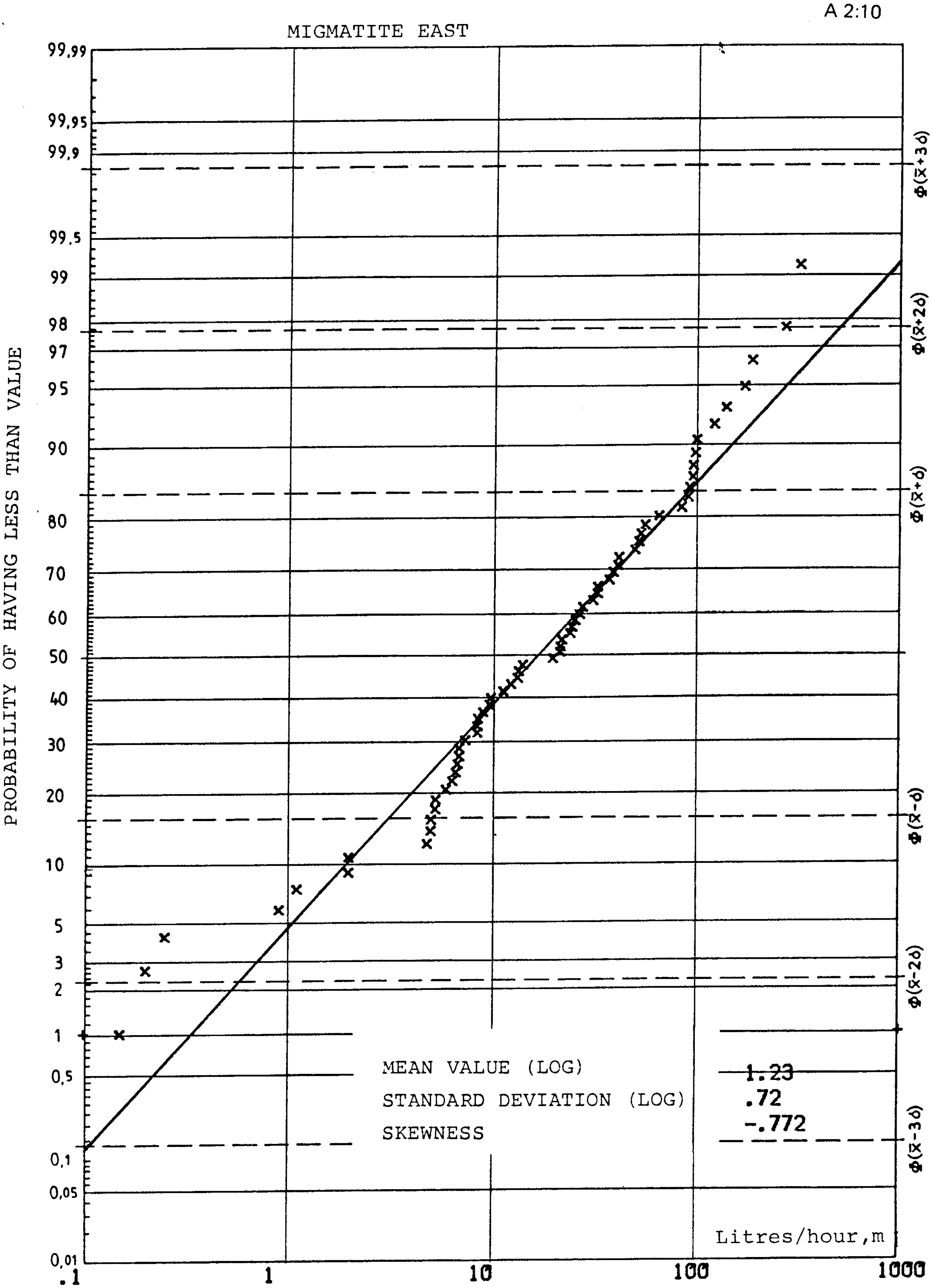

MIGMATITE EAST
PROBABILITY OF HAVING LESS THAN VALUE
99,99
99,95
99,9
99,5
99
98
97
95
90
80
70
60
50
40
30
20
10
5
3
2
1
0,5
0,1
0,05
0,01
.1
1
10
100
1000
Litres/hour,m
$\Phi(\bar{x}+3\sigma)$
$\Phi(\bar{x}+2\sigma)$
$\Phi(\bar{x}+\sigma)$
$\Phi(\bar{x}-\sigma)$
$\Phi(\bar{x}-2\sigma)$
$\Phi(\bar{x}-3\sigma)$
MEAN VALUE (LOG) 1.23
STANDARD DEVIATION (LOG) .72
SKEWNESS -.772

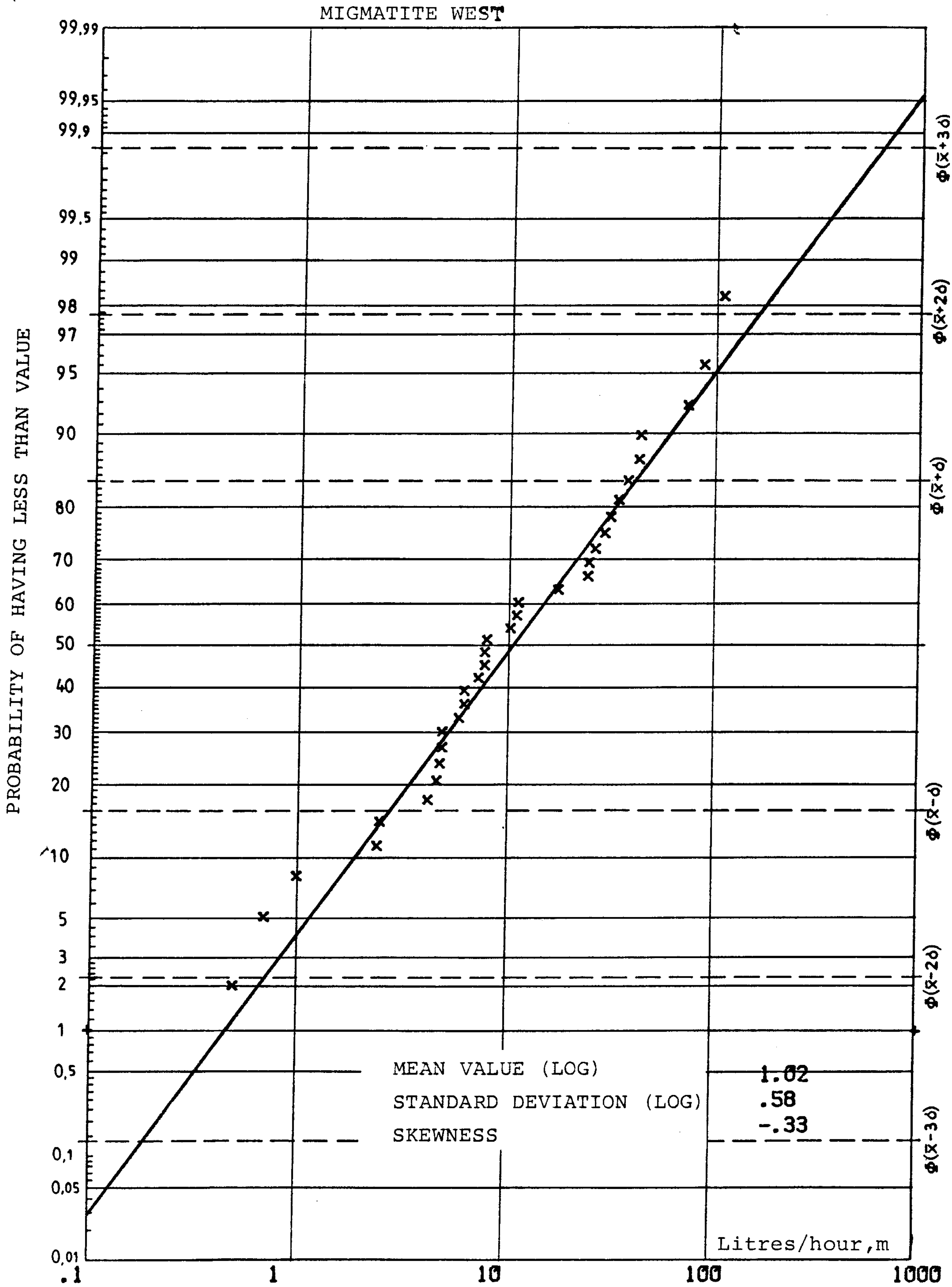

MIGMATITE WEST
PROBABILITY OF HAVING LESS THAN VALUE
99,99
99,95
99,9
99,5
99
98
97
95
90
80
70
60
50
40
30
20
10
5
3
2
1
0,5
0,1
0,05
0,01
.1
1
10
100
1000
Litres/hour,m
MEAN VALUE (LOG) 1.02
STANDARD DEVIATION (LOG) .58
SKEWNESS -.33
Φ(x̄+3σ)
Φ(x̄+2σ)
Φ(x̄+σ)
Φ(x̄-σ)
Φ(x̄-2σ)
Φ(x̄-3σ)

APPENDIX 3

Hydraulic conductivity values from the injection tests and classification

TECTONIC ELEMENTS	CODE
TENSION N-S T1	T1
TENSION E-W T2	T2
SHEAR FRACTURES	S
UNDEFORMED PARTS OF BLOCKS	B

Table Core drilling Gi 1, Hydraulic Conductivity (K)
25 m and 5 m sealed off sections

Section (m)	Depth	K (m/s)	Code	Section (m)	K (m/s)
10 - 35	22.5	2.2×10^{-7}	B	185 - 190	u.m.
35 - 60	47.5	1.1×10^{-7}	B	190 - 195	9.3×10^{-7}
60 - 85	72.5	3.2×10^{-8}	B	195 - 200	u.m.
85 - 110	97.5	u.m.	B	200 - 205	u.m.
110 - 135	122.5	1.7×10^{-11}	B	205 - 210	u.m.
135 - 160	147.5	1.6×10^{-10}	B		
160 - 185	172.5	8.6×10^{-10}	B	275 - 280	6.9×10^{-7}
185 - 210	197.5	1.3×10^{-7}	B	280 - 285	u.m.
210 - 235	222.5	u.m.	B		
235 - 260	247.5	3.6×10^{-9}	B	385 - 390	u.m.
260 - 285	272.5	2.1×10^{-8}	B	390 - 395	u.m.
285 - 310	297.5	1.4×10^{-11}	B		
310 - 335	322.5	u.m.	B	460 - 465	u.m.
335 - 360	347.5	u.m.	B	465 - 470	u.m.
360 - 385	372.5	u.m.	B		
385 - 410	397.5	u.m.	B	500 - 505	5.6×10^{-10}
410 - 435	422.5	u.m.	B	505 - 510	u.m.
435 - 460	447.5	u.m.	B		
460 - 485	472.5	u.m.	B		u.m. $\leq 5.0 \times 10^{-11}$
485 - 510	497.5	1.6×10^{-10}	B		
510 - 535	522.5	u.m.	B		
535 - 560	547.5	3.0×10^{-11}	B		
560 - 585	572.5	u.m.	B		
585 - 610	597.5	u.m.	B		
610 - 635	622.5	u.m.	B		
635 - 660	647.5	u.m.	B		
660 - 685	672.5	u.m.	B		

u.m. $\leq 1.0 \times 10^{-11}$

u.m. = less or equal to limitation of equipment

Table Core drilling Gi 2 Hydraulic Conductivity (K)
25 m and 10 m sealed off sections

Section (m)	Depth	K (m/s)	Code	Section (m)	K (m/s)
33 - 58	39.4	5.6×10^{-8}	B	87.5- 97.5	1.3×10^{-6}
58 - 83	61.1	3.9×10^{-8}	B	97.5-107.5	2.5×10^{-6}
83 - 108	82.7	1.6×10^{-6}	B	175-185	2.8×10^{-7}
108 - 133	104.3	1.6×10^{-8}	B	210-220	8.1×10^{-7}
133 - 158	126.0	7.1×10^{-10}	T1	220-230	6.5×10^{-7}
158 - 183	147.6	1.3×10^{-7}	B	317.5-327.5	3.1×10^{-11}
181 - 206	167.6	1.1×10^{-7}	B	327.5-337.5	1.6×10^{-10}
206 - 231	189.2	1.1×10^{-6}	T2	395-405	(2.8×10^{-10})
231 - 256	210.9	8.7×10^{-8}	T2	410-420	(2.3×10^{-10})
256 - 281	232.5	1.2×10^{-7}	T2		
281 - 306	254.2	1.1×10^{-9}	T2		(K prel.)
303 - 328	273.2	5.9×10^{-10}	T2		
328 - 353	294.9	8.6×10^{-11}	B		
353 - 378	316.5	8.6×10^{-11}	B		
378 - 403	338.2	1.0×10^{-10}	B		
403 - 428	360.0	1.2×10^{-8}	B		
428 - 453	381.5	8.8×10^{-11}	B		
453 - 478	403.1	2.6×10^{-11}	B		
478 - 503	424.8	3.1×10^{-10}	T1		
503 - 528	446.4	8.6×10^{-10}	T1		
528 - 553	468.1	2.1×10^{-11}	T1		
553 - 578	489.7	4.2×10^{-11}	B		
578 - 603	511.4	2.0×10^{-11}	B		
603 - 628	533.0	4.5×10^{-11}	B		
628 - 653	554.7	1.1×10^{-11}	B		
653 - 678	576.4	4.6×10^{-12}	B		

Table Core drilling Gi 3 Hydraulic Conductivity (K)
25 m and 5 m sealed off sections

Section (m)	Depth	K (m/s)	Code	Section (m)	K (m/s)
10 - 35	19.5	2.1×10^{-7}	T2	185 - 190	1.6×10^{-9}
35 - 60	41.2	7.8×10^{-8}	S	223 - 228	u.m.
60 - 85	62.8	2.0×10^{-7}	T2	360 - 365	2.6×10^{-12}
85 - 110	84.4	1.1×10^{-9}	S	365 - 370	2.9×10^{-11}
110 - 135	106.1	5.5×10^{-9}	S	370 - 375	u.m.
135 - 160	127.7	8.8×10^{-9}	B	375 - 380	2.6×10^{-9}
160 - 185	149.4	7.9×10^{-11}	B	380 - 385	u.m.
185 - 210	171.0	2.3×10^{-10}	B		
210 - 235	192.7	7.6×10^{-11}	B	u.m. $\leq$	2.5×10^{-11}
235 - 260	214.3	3.2×10^{-10}	B		
260 - 285	236.0	2.2×10^{-9}	B		
285 - 310	257.6	1.4×10^{-11}	B		
310 - 335	279.3	1.2×10^{-11}	B		
335 - 360	300.9	2.5×10^{-11}	B		
360 - 385	322.6	4.1×10^{-10}	B		
385 - 410	344.2	u.m.	T2		
410 - 435	365.9	u.m.	T2		
435 - 460	387.5	u.m.	B		
460 - 485	409.2	4.0×10^{-9}	B		
485 - 510	430.8	9.8×10^{-9}	B		
510 - 535	452.5	3.4×10^{-9}	T1		
535 - 560	474.1	u.m.	T1		
560 - 585	495.8	u.m.	T1		
585 - 610	517.5	1.2×10^{-8}	T2		
610 - 635	539.2	1.3×10^{-9}	T2		
635 - 660	560.8	u.m.	B		
660 - 685	582.5	1.0×10^{-10}	B		

u.m. $\leq 5.0 \times 10^{-12}$

u.m. = less or equal to limitation of equipment

Table Core drilling Gi4 Hydraulic Conductivity (K)
25 m and 5 m sealed off sections

Section (m)	Depth	K (m/s)	Code	Section (m)	K (m/s)
20 - 45	30.5	2.02×10^{-8}	B	220 - 225	1.0×10^{-8}
45 - 70	54.0	1.41×10^{-6}	B	225 - 230	6.6×10^{-10}
70 - 95	77.5	2.99×10^{-10}	B	240 - 245	1.5×10^{-9}
95 - 120	101.0	4.35×10^{-8}	B	245 - 250	1.1×10^{-6}
120 - 145	124.5	1.83×10^{-9}	B	250 - 255	3.8×10^{-11}
145 - 170	148.0	1.64×10^{-8}	T2		
170 - 195	171.5	1.91×10^{-9}	T2	400 - 405	u.m.
195 - 225	194.9	1.96×10^{-11}	B	405 - 410	1.2×10^{-8}
220 - 245	218.5	2.08×10^{-8}	B	403 - 408	u.m.
245 - 270	241.9	5.77×10^{-9}	B		
270 - 295	265.5	4.22×10^{-11}	T1		u.m. $\leq 2.5 \times 10^{-11}$
295 - 320	288.9	u.m.	T1		
320 - 345	312.4	u.m.	T1		
345 - 370	335.9	u.m.	B		
370 - 395	359.4	u.m.	B		
395 - 420	382.9	2.28×10^{-9}	B		
420 - 445	406.4	u.m.	B		
445 - 470	429.9	u.m.	B		
470 - 495	453.4	u.m.	B		
495 - 520	476.8	9.46×10^{-12}	B		
520 - 545	500.4	3.16×10^{-11}	B		
545 - 570	523.8	1.1×10^{-9}	B		
570 - 595	547.4	u.m.	B		
595 - 620	570.9	3.88×10^{-11}	S		
620 - 645	594.7	1.7×10^{-11}	S		
645 - 670	617.8	1.04×10^{-10}	B		

u.m. $\leq 5.0 \times 10^{-12}$

u.m. = less or equal to limitation of equipment

Table Core drilling Gi 5 Hydraulic Conductivity (K)
25 and 10 m sealed off sections

Section (m)	Depth	K (m/s)	Code	Section (m)	K (m/s)
20 - 45	28.1	2.74×10^{-7}	B	225 - 235	9.31×10^{-6}
45 - 70	49.8	1.97×10^{-7}	B	235 - 245	4.49×10^{-9}
70 - 95	71.4	7.71×10^{-8}	B		
95 - 120	93.1	9.02×10^{-7}	B	250 - 260	1.80×10^{-7}
120 - 145	114.7	5.68×10^{-6}	T1	290 - 300	3.04×10^{-10}
145 - 170	136.4	4.78×10^{-6}	T1	320 - 330	1.70×10^{-8}
170 - 195	158.0	1.65×10^{-7}	B	335 - 345	2.3×10^{-10}
195 - 220	179.7	1.09×10^{-10}	B		
220 - 245	201.3	2.33×10^{-6}	T2	530 - 540	1.42×10^{-11}
245 - 270	222.9	1.02×10^{-7}	B	540 - 550	u.m.
270 - 295	244.6	2.2×10^{-11}	B		
295 - 320	266.3	4.34×10^{-10}	B	u.m. $\leq$	1.3×10^{-11}
320 - 345	287.9	1.13 x 10-8	B		
345 - 370	309.6	2.08×10^{-10}	B		
370 - 395	331.2	1.60×10^{-11}	B		
395 - 420	352.9	2.56×10^{-11}	T1	520 - 702	1.41×10^{-12}
420 - 445	374.5	2.85×10^{-11}	T1		
445 - 470	396.2	u.m.	T2		
470 - 495	417.8	u.m.	B		
495 - 520	439.5	u.m.	B		
515 - 540	465.8	2.34×10^{-11}	B		
u.m. $\leq$	$5.0 \times$	10^{-12}			

u.m. = less or equal to limitation of equipment

Table Core drilling Gi 6 Hydraulic Conductivity (K)
25 m sealed off sections

Section (m)	Depth	K (m/s)	Code
10 - 35	19.5	1.94×10^{-8}	B
35 - 60	41.2	9.59×10^{-8}	B
60 - 85	62.7	7.89×10^{-8}	B
85 - 110	84.4	u.m.	B
110 - 135	106.1	6.39×10^{-8}	B
135 - 160	127.7	1.80×10^{-7}	T1
160 - 185	149.4	1.59×10^{-10}	T1
185 - 210	171.0	u.m.	T2
210 - 235	192.7	u.m.	T2
235 - 260	214.3	u.m.	B
260 - 285	236.6	u.m.	B
285 - 310	257.6	u.m.	B
310 - 335	279.3	u.m.	B
335 - 360	300.9	u.m.	B
360 - 385	322.6	u.m.	T2
385 - 410	344.2	u.m.	T2
410 - 435	365.9	u.m.	T2
435 - 460	387.2	4.01×10^{-11}	B
460 - 485	409.2	u.m.	B
485 - 510	430.8	1.07×10^{-11}	S
510 - 535	452.5	u.m.	S
535 - 560	474.1	u.m.	B
560 - 585	495.8	u.m.	B
585 - 610	517.5	1.06×10^{-11}	T1
610 - 635	539.2	u.m.	B
635 - 660	560.8	1.44×10^{-11}	B

u.m. $\leq 1.0 \times 10^{-11}$

u.m. = less or equal to limitation of equipment

Table Core drilling Gi 7 Hydraulic Conductivity (K)
25 m and 5 m sealed off sections

Section (m)	Depth	K (m/s)	Code	Section (m)	K (m/s)
10 - 35	19.5	1.43×10^{-7}	B	210 - 215	5.19×10^{-10}
35 - 60	41.2	9.51×10^{-8}	B	225 - 230	1.84×10^{-7}
60 - 85	62.2	9.21×10^{-9}	B	230 - 235	2.6×10^{-8}
85 - 110	84.4	4.82×10^{-9}	B	235 - 240	9.70×10^{-9}
110 - 135	106.1	1.29×10^{-9}	B	335 - 340	7.48×10^{-11}
135 - 160	127.7	4.69×10^{-6}	B	345 - 350	1.13×10^{-9}
160 - 185	149.4	5.40×10^{-7}	B	350 - 355	1.9×10^{-12}
185 - 210	171.0	1.75×10^{-10}	B	460 - 465	1.74×10^{-10}
210 - 235	192.7	2.86×10^{-8}	B	570 - 575	u.m.
235 - 260	214.3	7.73×10^{-9}	B	580 - 585	1.53×10^{-8}
260 - 285	236.6	1.15×10^{-9}	B	595 - 600	u.m.
285 - 310	257.6	2.27×10^{-11}	B		
310 - 335	279.3	4.86×10^{-11}	B		u.m. $\leqslant 2.5 \times 10^{-11}$
335 - 360	300.9	1.94×10^{-9}	T2		
360 - 385	322.6	1.08×10^{-11}	T2		
385 - 410	344.2	7.54×10^{-12}	T2		
410 - 435	365.9	5.47×10^{-12}	B		
435 - 460	387.2	7.75×10^{-10}	B		
460 - 485	409.2	4.75×10^{-10}	B		
485 - 510	430.8	4.70×10^{-12}	B		
510 - 535	452.5	6.37×10^{-12}	B		
535 - 560	474.1	u.m.	B		
560 - 585	495.2	4.76×10^{-9}	T2		
585 - 610	517.5	5.98×10^{-9}	T2		
610 - 635	539.2	u.m.	B		
635 - 660	560.8	1.02×10^{-11}	B		
660 - 685	582.5	u.m.			

u.m. $\leqslant 5.0 \times 10^{-12}$

u.m. = less or equal to limitation of equipment

Table Core drilling Gi 8 Hydraulic Conductivity (K)
25 m and 5 m sealed off sections

Section (m)	Depth	K (m/s)	Code	Section (m)	K (m/s)
20 - 45	28.7	3.18×10^{-8}	B	325 - 330	1.21×10^{-8}
45 - 70	50.8	7.36×10^{-10}	B	330 - 335	2.50×10^{-9}
70 - 95	72.8	1.10×10^{-10}	S	335 - 340	1.11×10^{-10}
95 - 120	94.9	7.39×10^{-11}	S	340 - 345	1.22×10^{-10}
120 - 145	116.9	6.48×10^{-11}	B	345 - 350	5.51×10^{-10}
145 - 170	139.0	1.48×10^{-9}	B	420 - 425	1.15×10^{-8}
170 - 195	161.1	6.00×10^{-8}	B	425 - 430	1.88×10^{-9}
195 - 220	183.2	4.86×10^{-9}	B	430 - 435	5.64×10^{-9}
220 - 245	205.3	u.m.	T1	450 - 455	u.m.
245 - 270	227.4	u.m.	T1	455 - 460	u.m.
270 - 295	249.4	1.45×10^{-11}	B	570 - 575	u.m.
295 - 320	271.5	4.10×10^{-11}	B	620 - 625	u.m.
320 - 345	293.6	1.42×10^{-8}	T2		
345 - 370	315.7	7.17×10^{-11}	B		u.m. $\leq 2.5 \times 10^{-11}$
370 - 395	337.7	2.90×10^{-11}	B		
395 - 420	359.8	2.25×10^{-11}	B		
420 - 445	381.8	2.27×10^{-9}	T1		
445 - 470	403.9	3.47×10^{-10}	T2		
470 - 495	426.0	u.m.	T2		
495 - 520	448.1	u.m.	B		
520 - 545	470.2	u.m.	B		
545 - 570	492.2	5.38×10^{-12}	B		
570 - 595	514.3	u.m.	B		
595 - 620	536.4	u.m.	T1		
620 - 645	558.5	u.m.	B		
645 - 670	580.5	u.m.	B		
670 - 695	602.6	u.m.	B		

u.m. $\leq 5.0 \times 10^{-12}$

u.m. = less or equal to limitation of equipment

Table Core drilling Gi 10 Hydraulic conductivity (K)
25 m and 5 m sealed off sections

Section (m)	Depth	K (m/s)	Code	Section	K (m/s)
20 - 45	29.5	8.40×10^{-8}	T1	135 - 140	1.99×10^{-10}
45 - 70	52.2	1.14×10^{-8}	B	285 - 290	1.89×10^{-7}
70 - 95	74.8	1.01×10^{-8}	B	290 - 295	u.m.
95 - 120	97.5	2.10×10^{-6}	B		
120 - 145	120.1	1.02×10^{-9}	B	470 - 475	9.61×10^{-11}
145 - 170	142.8	3.46×10^{-9}	B	475 - 480	4.00×10^{-11}
170 - 195	165.4	1.48×19^{-11}	B	480 - 485	6.42×10^{-10}
195 - 220	188.1	5.99×10^{-11}	B	485 - 490	4.23×10^{-11}
220 - 245	210.8	1.64×10^{-10}	S	490 - 495	u.m.
245 - 270	233.4	u.m.	S		
270 - 295	256.1	2.11×10^{-8}	S	500 - 505	1.07×10^{-9}
295 - 320	278.7	u.m.	B		
320 - 345	301.4	3.50×10^{-11}	B		
345 - 370	324.1	5.12×10^{-9}	B	u.m. $\leqslant 2.5 \times 10^{-11}$	
370 - 395	346.7	3.85×10^{-10}	B		
395 - 420	369.4	u.m.	B	Single packer	
420 - 445	392.0	u.m.	B	595 - 702	2.86×10^{-11}
445 - 470	414.7	8.26×10^{-12}	T1		
470 - 495	437.3	3.75×10^{-8}	T2		
495 - 520	460.0	2.50×10^{-10}	T2		
520 - 545	482.6	u.m.	B		
545 - 570	505.3	u.m.	B		
570 - 595	528.0	3.09×10^{-11}	B		
595 - 620	550.6	u.m.	B		
620 - 645	573.3	u.m.	S		
645 - 670	595.9	u.m.	B		
670 - 695	618.6	u.m.	B		

u.m. $\leqslant 5.0 \times 10^{-12}$

u.m. = less or equal to limitation of equipment

Table Core drilling Gi 11 Hydraulic conductivity (K)
25 and 5 m sealed off sections

Section (m)	Depth	K (m/s)	Code	Section (m)	K (m/s)
20 - 45	29.5	7.28×10^{-9}	B	225 - 230	1.26×10^{-9}*
45 - 70	52.2	2.37×10^{-9}*	B	230 - 235	1.22×10^{-9}*
70 - 95	74.8	1.98×10^{-7}	B	235 - 240	3.89×10^{-10}
95 - 120	97.5	2.3×10^{-9}	B	240 - 245	3.49×10^{-9}
120 - 145	120.1	1.36×10^{-10}*	B	245 - 250	9.24×10^{-8}
145 - 170	142.8	1.45×10^{-10}	B	250 - 255	3.40×10^{-10}
170 - 195	165.4	6.10×10^{-11}*	B	270 - 275	8.16×10^{-11}
195 - 220	188.1	4.92×10^{-11}	B	320 - 325	u.m.
220 - 245	210.8	7.97×10^{-10}	B	325 - 330	8.30×10^{-9}
245 - 270	233.4	1.81×10^{-8}	B	330 - 335	u.m.
270 - 295	256.1	1.52×10^{-9}	B	440 - 445	7.31×10^{-9}*
295 - 320	278.7	4.79×10^{-12}	B		
320 - 345	301.4	1.03×10^{-9}	T2		
345 - 370	324.1	1.83×10^{-11}*	B		
370 - 395	346.7	2.63×10^{-11}	S		u.m. $\leq 2.5 \times 10^{-11}$
395 - 420	369.4	5.41×10^{-12}	B		
420 - 445	392.0	1.68×10^{-9}	T2		
445 - 470	414.7	u.m.	B		
470 - 495	437.3	6.57×10^{-11}	B		
495 - 520	460.0	6.88×10^{-11}*	B		
520 - 545	482.6	2.94×10^{-11}	B		
545 - 570	505.3	u.m.	B		
570 - 595	528.0	u.m.	B		
595 - 620	550.6	u.m.	B		
620 - 645	573.3	2.65×10^{-10}	B		
645 - 670	595.9	u.m.	B		
670 - 695	618.6	u.m.	S		

u.m. $\leq 5.0 \times 10^{-12}$

u.m. = less or equal to limitation of equipment

* Calculated according to Banks with constant of Moyes

Table Core drilling Gi 13 Hydraulic Conductivity (K)
25 m and 5 m sealed off sections

Section (m)	Depth	K (m/s)	Code	Section (m)	K (m/s)
15 - 40	24.1	9.65×10^{-7}	B	240 - 245	u.m.
40 - 65	49.9	1.70×10^{-7}	B	245 - 250	4.18×10^{-9}
65 - 90	67.8	6.50×10^{-7}	T1	250 - 255	3.32×10^{-9}
90 - 115	89.6	1.6×10^{-5}	T1	265 - 270	4.97×10^{-7}
115 - 140	111.5	2.56×10^{-7}	B	275 - 280	7.24×10^{-7}
140 - 165	133.4	6.82×10^{-9}	B	280 - 285	9.60×10^{-7}
165 - 190	155.2	4.60×10^{-11}	B	515 - 520	2.15×10^{-7}*
190 - 215	177.1	3.57×10^{-11}	B	525 - 530	1.83×10^{-7}*
215 - 240	198.9	1.23×10^{-11}	B	535 - 540	7.17×10^{-10}*
240 - 265	220.8	2.85×10^{-9}	T2		
265 - 290	242.7	1.42×10^{-8}	T1		
290 - 315	264.6	1.36×10^{-11}	B		
315 - 340	286.4	1.30×10^{-11}	B		
340 - 365	308.3	1.24×10^{-11}	B		
365 - 390	330.2	1.19×10^{-11}	B		
390 - 415	352.0	7.69×10^{-12}	B		
415 - 440	373.0	2.54×10^{-11}	B		
440 - 465	395.8	2.24×10^{-9}	T2		
465 - 490	417.6	2.10×10^{-11}	B		
490 - 515	439.5	7.11×10^{-12}	B		
515 - 540	461.4	1.05×10^{-7}	T2		
540 - 565	483.2	u.m.	B		
565 - 590	505.1	u.m.	B		
590 - 615	526.9	u.m.	B		
615 - 640	548.8	1.47×10^{-10}*	B		
640 - 665	570.7	u.m.	B		
665 - 690	592.6	u.m.	B		

u.m. $\leq 2.5 \times 10^{-11}$ (5 m sections)

u.m. $\leq 5.0 \times 10^{-12}$

u.m. = less or equal to limitation of equipment

* Calculated according to Banks with constant of Moyes

APPENDIX 4

Drawings

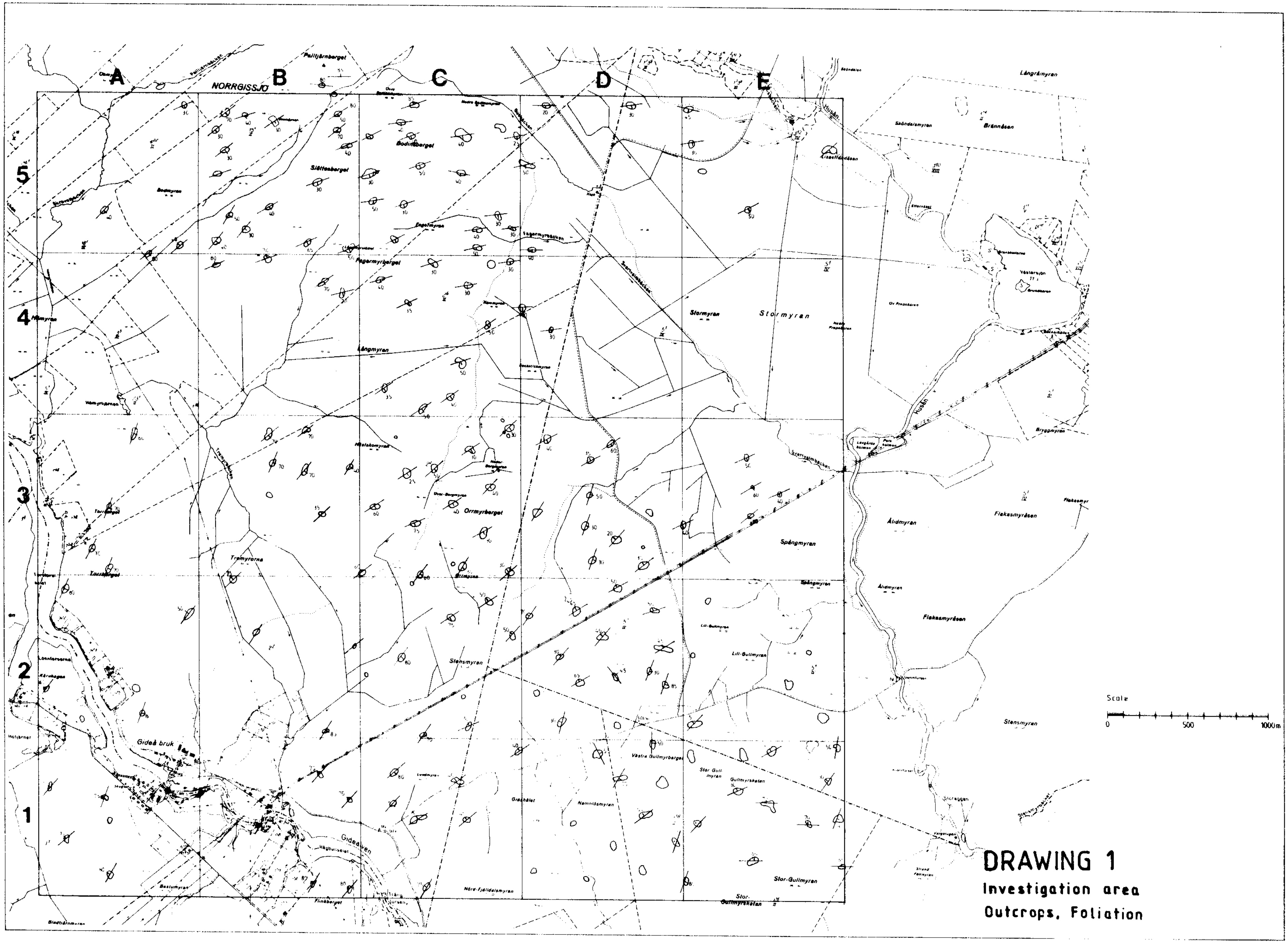

DRAWING 1

Investigation area

Outcrops, Foliation

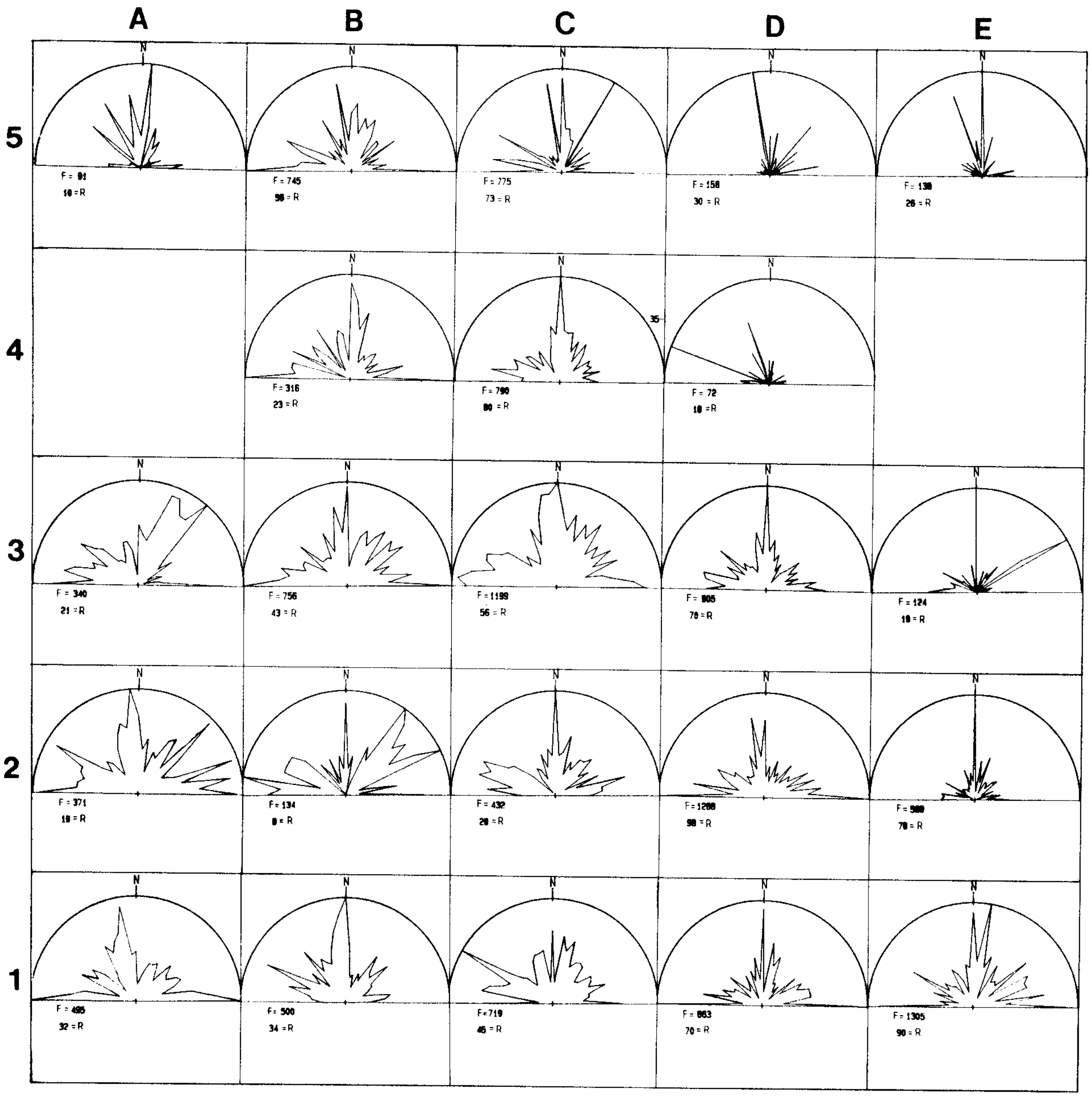

LEGEND:

F = 100 —— 100 EXISTING FRACTURES IN THE INVESTIGATED AREA

100 = R —— 100 FRACTURES CORRESPOND TO RADIUS

DRAWING 2

Rose diagrams

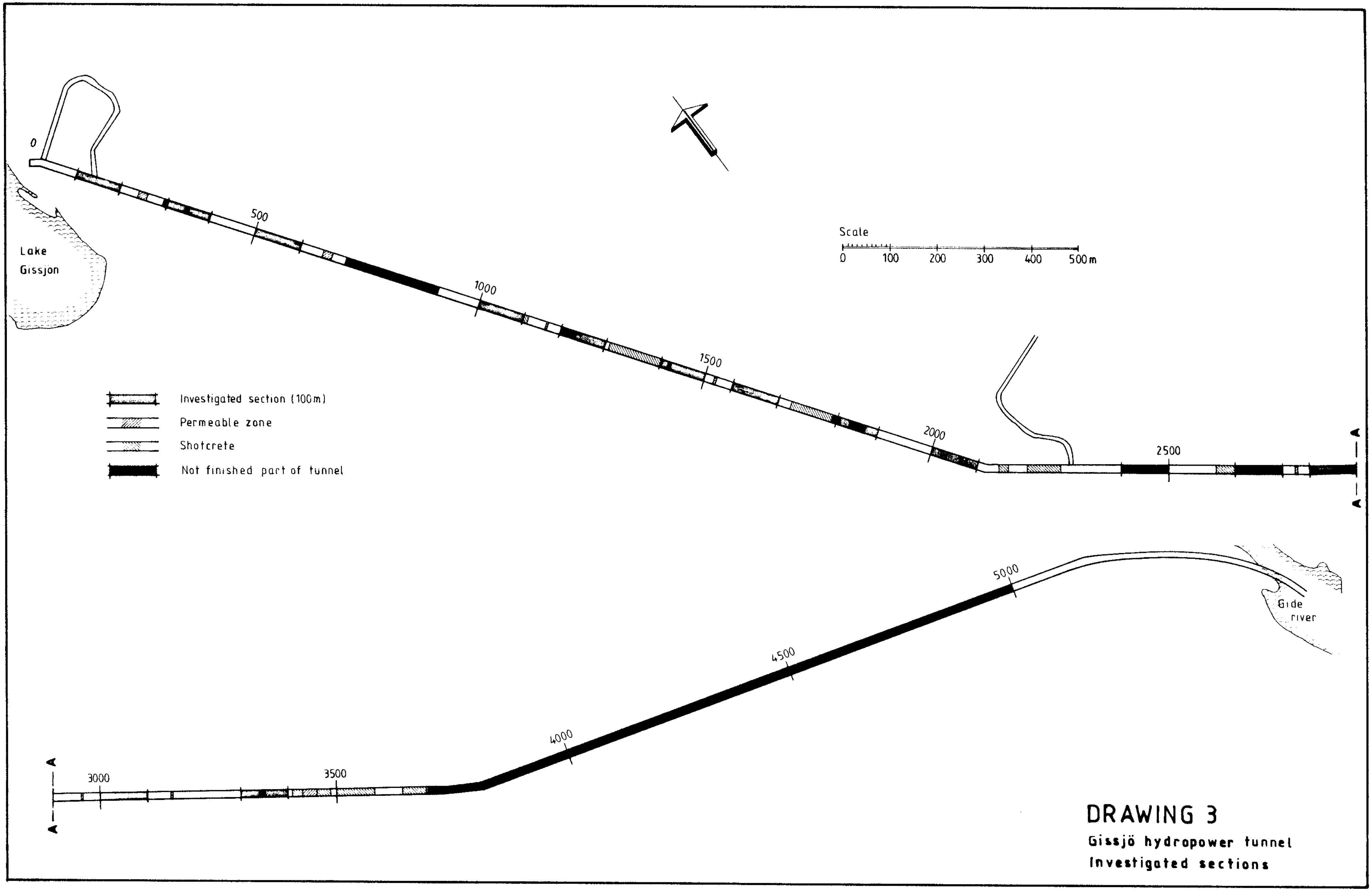

DRAWING 3

Gissjö hydropower tunnel
Investigated sections

Fractures in the Gissjö hydropower tunnel
Dips of inclined fractures in the most prominent strike sectors

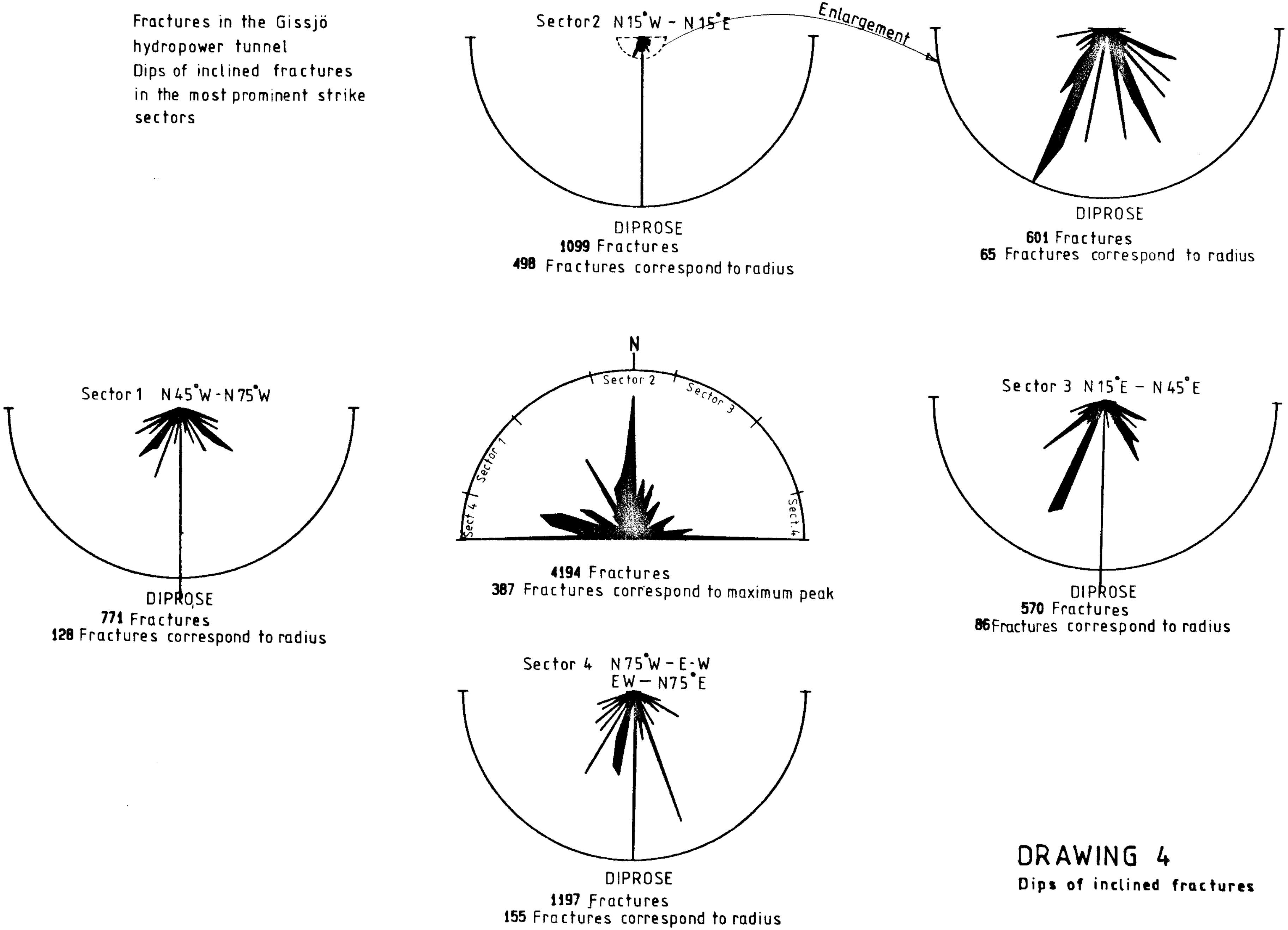

DRAWING 4
Dips of inclined fractures

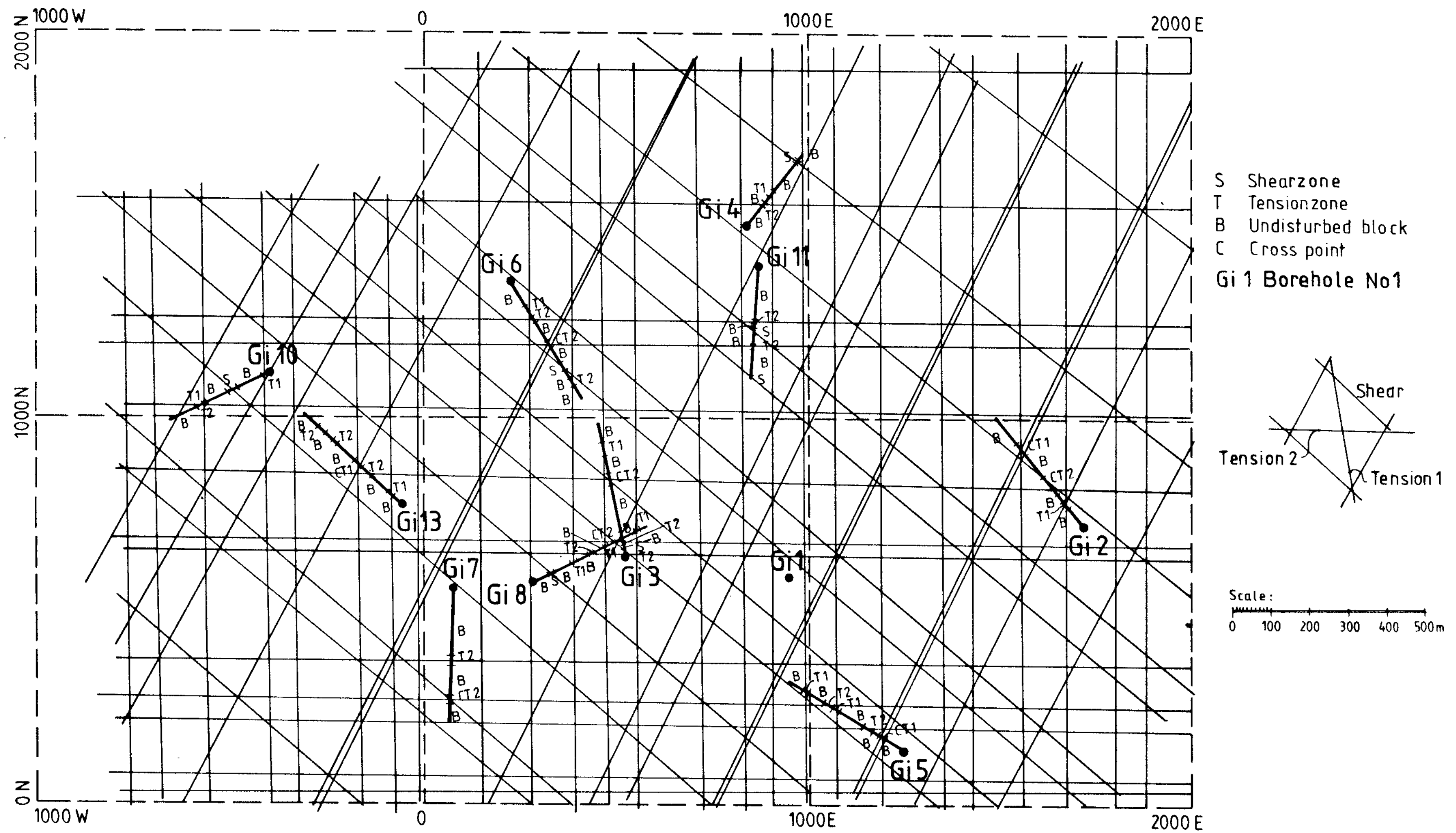

DRAWING 5

Tectonic model

Gideå "SGAB area"

Core drillings with injection test

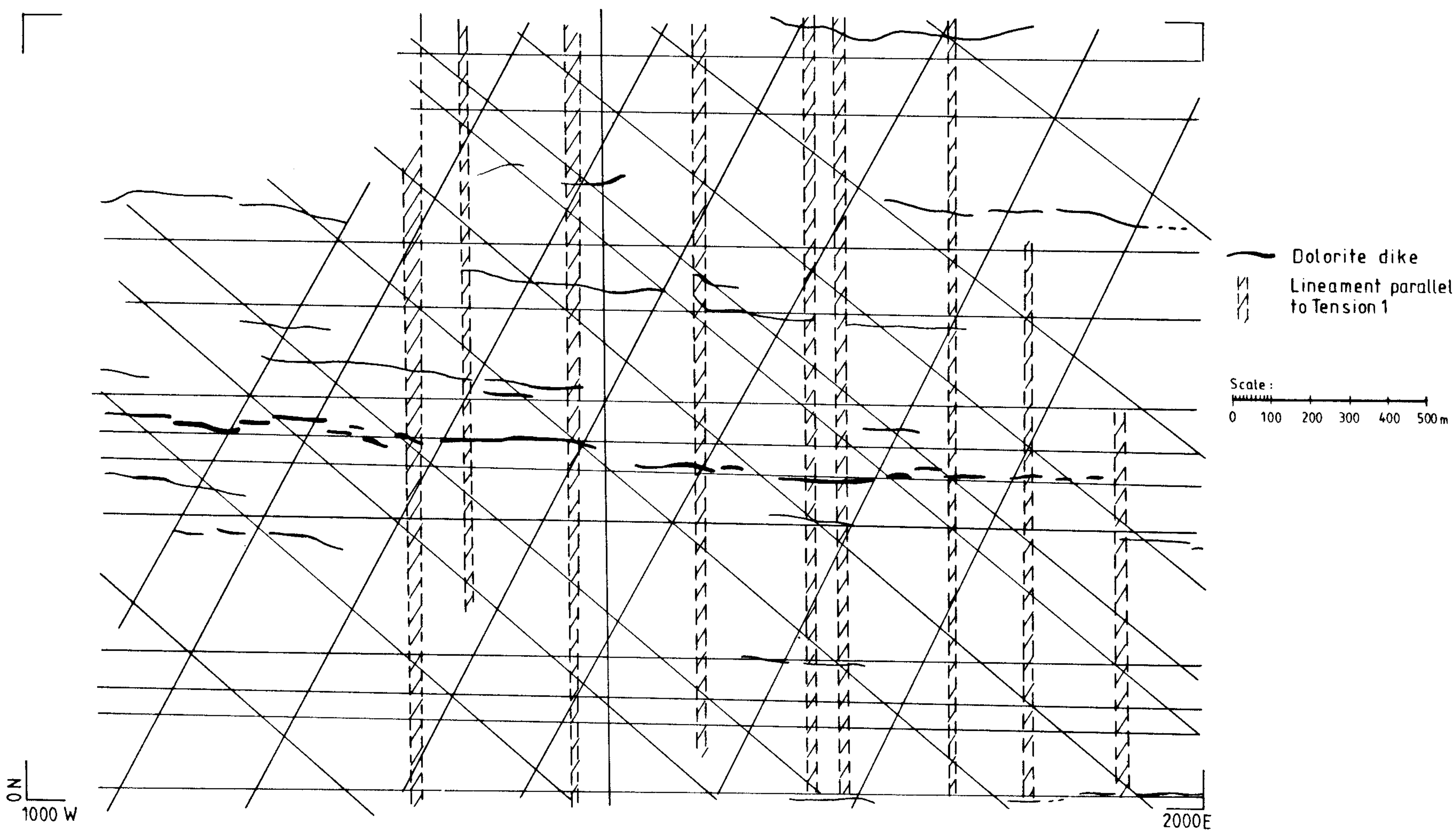

DRAWING 6

Interpretation from magnetic anomalies

List of SKB reports

Annual Reports

1977–78
TR 121
KBS Technical Reports 1 – 120.
Summaries. Stockholm, May 1979.

1979
TR 79–28
The KBS Annual Report 1979.
KBS Technical Reports 79-01 – 79-27.
Summaries. Stockholm, March 1980.

1980
TR 80–26
The KBS Annual Report 1980.
KBS Technical Reports 80-01 – 80-25.
Summaries. Stockholm, March 1981.

1981
TR 81–17
The KBS Annual Report 1981.
KBS Technical Reports 81-01 – 81-16.
Summaries. Stockholm, April 1982.

1982
TR 82–28
The KBS Annual Report 1982.
KBS Technical Reports 82-01 – 82-27.
Summaries. Stockholm, July 1983.

1983
TR 83–77
The KBS Annual Report 1983.
KBS Technical Reports 83-01 – 83-76
Summaries. Stockholm, June 1984.

1984
TR 85–01
Annual Research and Development Report 1984
Including Summaries of Technical Reports Issued during 1984. (Technical Reports 84-01 – 84-19)
Stockholm June 1985.

1985
TR 85-20
Annual Research and Development Report 1985
Including Summaries of Technical Reports Issued during 1985. (Technical Reports 85-01-85-19)
Stockholm May 1986.

Technical Reports

1986

TR 86-01
I: An analogue validation study of natural radionuclide migration in crystalline rock using uranium-series disequilibrium studies
II: A comparison of neutron activation and alpha spectroscopy analyses of thorium in crystalline rocks
J A T Smellie, Swedish Geological Co, A B MacKenzie and R D Scott, Scottish Universities Research Reactor Centre
February 1986

TR 86-02
Formation and transport of americium pseudocolloids in aqueous systems
U Olofsson
Chalmers University of Technology, Gothenburg, Sweden
B Allard
University of Linköping, Sweden
March 26, 1986

TR 86-03
Redox chemistry of deep groundwaters in Sweden
D Kirk Nordstrom
US Geological Survey, Menlo Park, USA
Ignasi Puigdomenech
Royal Institute of Technology, Stockholm, Sweden
April 1, 1986

TR 86-04
Hydrogen production in alpha-irradiated bentonite
Trygve Eriksen
Royal Institute of Technology, Stockholm, Sweden
Hilbert Christensen
Studsvik Energiteknik AB, Nyköping, Sweden
Erling Bjergbakke
Risö National Laboratory, Roskilde, Denmark
March 1986

TR 86-05
Preliminary investigations of fracture zones in the Brändan area, Finnsjön study site
Kaj Ahlbom, Peter Andersson, Lennart Ekman, Erik Gustafsson, John Smellie,
Swedish Geological Co, Uppsala
Eva-Lena Tullborg, Swedish Geological Co, Göteborg
February 1986

TR 86-06
Geological and tectonic description of the Klipperås study site
Andrzej Olkiewicz
Vladislav Stejskal
Swedish Geoloaical Company
Uppsala, October, 1986

TR 86-07
Geophysical investigations at the Klipperås study site
Stefan Sehlstedt
Leif Stenberg
Swedish Geological Company
Luleå, July 1986

TR 86-08
Hydrogeological investigations at the Klipperås study site
Bengt Gentzschein
Swedish Geological Company
Uppsala, June 1986

TR 86-09
Geophysical laboratory investigations on core samples from the Klipperås study site
Leif Stenberg
Swedish Geological Company
Luleå, July 1986

TR 86-10
Fissure fillings from the Klipperås study site
Eva-Lena Tullborg
Swedish Geological Company
Göteborg, June 1986

TR 86-11
Hydraulic fracturing rock stress measurements in borehole Gi-1, Gideå Study Site, Sweden
Bjarni Bjarnason and Ove Stephansson
Division of Rock Mechanics,
Luleå University of Technology, Sweden
April 1986

TR 86-12
PLAN 86— Costs for management of the radioactive waste from nuclear power production
Swedish Nuclear Fuel and Waste Management Co
June 1986

TR 86-13
Radionuclide transport in fast channels in crystalline rock
Anders Rasmuson, Ivars Neretnieks
Department of Chemical Engineering
Royal Institute of Technology, Stockholm
March 1985

TR 86-14
Migration of fission products and actinides in compacted bentonite
Börje Torstenfelt
Department of Neclear Chemistry, Chalmers University of Technology, Göteborg
Bert Allard
Department of water in environment and society, Linköping university, Linköping
April 24, 1986

TR 86-15
Biosphere data base revision
Ulla Bergström, Karin Andersson, Björn Sundblad, Studsvik Energiteknik AB, Nyköping
December 1985

TR 86-16
Site investigation
Equipment for geological, geophysical, hydrogeological and hydrochemical characterization
Karl-Erik Almén, SKB, Stockholm
Olle Andersson, IPA-Konsult AB, Oskarshamn
Bengt Fridh, Bengt-Erik Johansson,
Mikael Sehlstedt, Swedish Geological Co, Malå
Erik Gustafsson, Kenth Hansson, Olle Olsson,
Swedish Geological Co, Uppsala
Göran Nilsson, Swedish Geological Co, Luleå
Karin Axelsen, Peter Wikberg, Royal Institute of Technology, Stocholm
November 1986

TR 86-17
Analysis of groundwater from deep boreholes in Klipperås
Sif Laurent
IVL, Swedish Environmental
Research Institute
Stockholm, 1986-09-22

TR 86-18
Technology and costs for decommissioning the Swedish nuclear power plants.
Swedish Nuclear Fuel and Waste Management Co
May 1986